(6)

CLASSIFICATION OF THIS PAGE

REPORT DOCUMENTATION PAGE

Form Approved
OMB No. 0704-0188

RT SECURITY CLASSIFICATION	1b. RESTRICTIVE MARKINGS
RITY CLASSIFICATION AUTHORITY	3. DISTRIBUTION/AVAILABILITY OF REPORT Aporoved for public release; distribution unlimited.
ASSIFICATION/DOWNGRADING SCHEDULE Unclassified	
RMING ORGANIZATION REPORT NUMBER(S) N00014-79-C-0647	5. MONITORING ORGANIZATION REPORT NUMBER(S)
IE OF PERFORMING ORGANIZATION Colorado State University	6b. OFFICE SYMBOL (If applicable)
	7a. NAME OF MONITORING ORGANIZATION
RESS (City, State, and ZIP Code) Department of Chemistry Fort Collins, CO 80523	7b. ADDRESS (City, State, and ZIP Code)
8a. NAME OF FUNDING/SPONSORING ORGANIZATION Office of Naval Research	8b. OFFICE SYMBOL (If applicable)
	9 PROCUREMENT INSTRUMENT IDENTIFICATION NUMBER N00014-79-C-0647
8c. ADDRESS (City, State, and ZIP Code) 800 North Quincy Street Arlington, VA 22217-5000	10. SOURCE OF FUNDING NUMBERS

PROGRAM ELEMENT NO	PROJECT NO	TASK NO	WORK UNIT ACCESSION NO

11 TITLE (Include Security Classification)
"7-Azaindole and its Clusters with Ar, CH_4, H_2O, NH_3, and Alcohols: Molecular Geometry and Nature of the First Excited Singlet Electronic State"

12 PERSONAL AUTHOR(S)
Seong K. Kim and E. R. Bernstein

13a TYPE OF REPORT	13b. TIME COVERED	14. DATE OF REPORT (Year, Month, Day)	15 PAGE COUNT
Technical Report	FROM _____ TO _____	December 15, 1989	

16 SUPPLEMENTARY NOTATION

17 COSATI CODES			18. SUBJECT TERMS (Continue on reverse if necessary and identify by block number)
FIELD	GROUP	SUB-GROUP	mass resolved, excitation vibronic spectra, jet cooled spectroscopy, 7-Azaindole, structure, clustering, pyrrole nitrogen, cyclic hydrogen bonded clusters, $n\pi^*$-$\pi\pi^*$ interaction;

19 ABSTRACT (Continue on reverse if necessary and identify by block number) planarity in S_0 and S_1

SEE ATTACHED ABSTRACT

20. DISTRIBUTION/AVAILABILITY OF ABSTRACT	21. ABSTRACT SECURITY CLASSIFICATION
☒ UNCLASSIFIED/UNLIMITED ☐ SAME AS RPT. ☐ DTIC USERS	Unclassified
22a NAME OF RESPONSIBLE INDIVIDUAL Elliot R. Bernstein	22b. TELEPHONE (Include Area Code) (303) 491-6347
	22c OFFICE SYMBOL

DD Form 1473, JUN 86 *Previous editions are obsolete.* SECURITY CLASSIFICATION OF THIS PAGE

S/N 0102-LF-014-6603

OFFICE OF NAVAL RESEARCH

Contract N00014-79-C-0647

TECHNICAL REPORT #66

"7-Azaindole and its Clusters with Ar, CH_4, H_2O, NH_3, and Alcohols: Molecular Geometry and Nature of the First Excited Singlet Electronic State"

by

Seong K. Kim and E. R. Bernstein

Accepted for publication in the

Journal of the American Chemical Society

Department of Chemistry
Colorado State University
Fort Collins, Colorado 80523

December 15, 1989

7-AZAINDOLE AND ITS CLUSTERS WITH Ar, CH_4, H_2O, NH_3, AND ALCOHOLS: MOLECULAR GEOMETRY, CLUSTER GEOMETRY, AND NATURE OF THE FIRST EXCITED SINGLET ELECTRONIC STATE

Seong K. Kim and Elliot R. Bernstein*

Chemistry Department
Colorado State University
Fort Collins, CO 80523

ABSTRACT

Mass resolved excitation vibronic spectra of jet-cooled 7-azaindole and its clusters with Ar, CH_4, NH_3, H_2O, D_2O, CH_3OH, and C_2H_5OH are reported and analyzed with regard to molecular and cluster geometry and the nature of the first excited singlet state. Large changes in the various spectra are observed upon clustering and upon deuteration of 7-azaindole. The observed vibronic spectra of both 7-azaindole and its clusters can be rationalized with two general assumptions: 1. the hydrogen attached to the pyrrole nitrogen of 7-azaindole is out of the molecular plane in the first excited singlet state; and 2. the observed spectra are characterized by strong $n\pi^* - \pi\pi^*$ mixing not completely removed by the clustering. MOPAC 5 calculations of molecular geometry suggest that the S_1 state is nonplanar. Additional cluster potential energy calculations suggest that the formation of cyclic hydrogen bonded clusters is not likely for these gas phase 1:1 or 1:2 7-azaindole/solvent clusters: the major gas phase solvent clustering probably takes place at the π-system of the 7-azaindole molecule.

I. INTRODUCTION

7-azaindole (see Figure 1a, 7AZI) is suggested to have two very interesting and important properties in solution: 1. when solvated by hydrogen bonding solvents (such as water, alcohols, ammonia, or even itself), it is thought to form a cyclic structure through a double hydrogen bond (Figure 1b)[1-3]; and 2. it will tautomerize (Figure 1c) in protic solvent solutions via a cyclic hydrogen bonded intermediate.[1,2,4-8] Such behavior is suggestive of the behavior of DNA bases[9], and thus 7AZI has been a particularly attractive and compelling system for study.

Spectra of isolated 7AZI, and/or 7AZI clustered with various hydrogen bonding and non-hydrogen bonding solvents should aid in the elucidation of the energetics and dynamics involved in both the cyclic hydrogen bonded solvation structures and in the tautomerization process. Supersonic jet expansion techniques coupled with laser spectroscopy and mass resolution (mass resolved excitation spectroscopy) are, of course, an excellent experimental approach to the study of molecular and cluster structure and energetics. Coupled with state of the art molecular orbital semiemperical calculations and potential energy cluster structure calculations, a good deal can be learned about bare molecule and cluster static and dynamic properties.[10-13]

Spectra of jet-cooled 7AZI, $(7AZI)_2$, and 7AZI/water clusters have been previously obtained with a view toward the interpretation of the tautomerization process.[14-16] The cluster spectra evidence large red shifts from the bare molecule spectrum and are quite complex: in general, the bare molecule and the various cluster spectra do not appear to coincide with regard to either vibronic structure or intensity. These observations were attributed to double hydrogen bonding such as shown in Figure 1. Nevertheless, aside from this explanation, no firm evidence exists for such structure in the gas phase. In fact, evidence from other theoretical and experimental studies of isolated van der Waals (vdW) clusters[10-13] strongly suggests that the major interaction between aromatic (solute) molecules and small solvent (i.e., H_2O, NH_3, C_nH_{2n+2}, ROH, etc.) molecules is through the π-electron system of the solute and the major electron density of the solvent. For systems with a substantial hydrogen bonding interaction in addition to the usual dispersion interaction, the cluster may have multiple stable structures: a planar hydrogen bonding

structure, a ring centered π-electron/electron density structure, and a compromise structure in which neither form of interaction dominates the geometry.

In addition to the above likely complications of multiple cluster geometries for 7AZI clusters and dimers, the isolated molecule may evidence its own complicated spectral behavior due to three potential causes: 1. mixing between nearly degenerate ^1L_a and ^1L_b ππ* excited electronic states; 2. mixing between the lowest ππ* state (probably ^1L_b which corresponds to the $^1B_{2u}$ state of benzene) and low lying nπ* states; and 3. nonplanarity of the 7AZI molecule in S_1 - in particular, at the pyrrole nitrogen. The ^1L_b state with its dipole parallel to the long axis of the molecule is rather insensitive to the solvent environment while the ^1L_a state is lowered in energy by polar environments. In the case of 7AZI, both transitions are polarized more or less along the long molecular axis.[17] The ^1L_a and ^1L_b states are well separated in gas phase indole[18] but are apparently close together in 7AZI.[1,19] For most isolated indole-like systems, only the ^1L_b state is identified at low energy. nπ* - ππ* interactions have not been reported or documented for 7AZI but have been suggested for purines[20] and other systems[21,22]. A rotational analysis of the 0_0^0 transition for $S_1 \leftarrow S_0$[23] does not suggest any nπ* - ππ* mixing but almost all the transition intensity is expected to be of a ππ* character.

The work reported in this paper addresses the above three complications for the S_1 state of bare and clustered 7AZI. Additionally, structures for 7AZI clusters with argon, methane, water, alcohols, and ammonia are suggested based on calculational and spectroscopic data.

II. EXPERIMENTAL PROCEDURES

A detailed description of the supersonic jet/laser apparatus is found in ref. 24. The doubled output of a pulsed Nd/YAG laser pumps a dye laser (R590, R610, KR620, R640, and SR640 plus DCM) whose output is in turn doubled into the ultraviolet in order to excite the samples of interest. The spectral range covered for a given sample often includes the output from several dyes so that

relative intensities must be calibrated in overlapping dye regions. For such situations, the intensities are noted in the figure captions.

Mass resolved excitation spectra (time-of-flight-mass spectroscopy-TOFMS) are obtained for all samples discussed in this report as the 7AZI (Aldrich, 98%) contains impurities that strongly absorb and emit light in the spectral regions of interest. These impurities could not be readily removed by recrystallization or vacuum sublimation. For the study of clusters, 2-color TOFMS are needed to obtain clear spectra of clusters of specific stoichiometry.

7AZI is placed inside the head of a pulsed supersonic nozzle heated to ca. 70°C. The expansion is generated using 50-70 psi of helium carrier gas. The solvents for clustering are either mixed with the carrier gas (gases) or placed in a trap before the nozzle.

d_1-7AZI (at the pyrrole ring nitrogen - H_{10} on N_1, see Figure 1) is synthesized by mixing 7AZI (1%) with D_2O at room temperature, extracting the d_1-7AZI with ether, and drying the organic component in vacuum. NMR spectra taken of the sample confirm that only the most acidic hydrogen (H_{10} of Figure 1) is replaced.

III. GEOMETRY OPTIMIZATION CALCULATIONS

The geometry of the 7AZI molecule is calculated for the S_0 and S_1 electronic states using the Molecular Orbital Package v. 5 (MOPAC 5)[25]. MOPAC 5 uses the semiempirical MNDO method with optimized parametric Hamiltonians AM1[26] and PM3[27]. With a given set of input data for bond lengths and angles, the program optimizes molecular geometry and point charge distributions over the atoms to obtain the minimum heat of formation. Additional molecular constants such as bond characteristics, dipole moment, and normal modes of vibration can also be found. These calculations are carried out for both the ground and first excited singlet states of 7AZI.

Two methods are employed to calculate the minimum energy geometries and binding energies for 7AZI/solvent clusters: the above MOPAC 5 program and a potential energy

calculation based on Lennard-Jones, hydrogen bonding, and coulomb atom-atom interactions.[28] These latter calculations are well described in our previous publications.[22]

Input data for the potential energy cluster calculations are the potential parameters for the different forms of interactions and different atoms, and the bond angles, bond lengths and atomic charges for all the molecules. These molecular data come from MOPAC 5 AM1 and PM3 Hamiltonian calculations.

IV. RESULTS AND DISCUSSION

A. 7-Azaindole - Spectroscopy

The 1-color TOFMS of 7AZI is presented in Figure 2. The intense feature at 34634 cm^{-1} is believed to be the $S_1 \leftarrow S_0$ transition origin. Low energy vibronic features, which play a major role in our overall analysis of the bare molecule and cluster spectra, are assigned at 234, 280, 306, 467, and 483 cm^{-1}. Prominent doublets are identified in this spectrum at 714, 718 cm^{-1} and 730, 735 cm^{-1} and an intense feature is located at 934 cm^{-1}. Upon deuteration of 7AZI at the acidic H_{10} position (d_1 - 7AZI) two changes are found in the 7AZI spectrum: 1. many of the low frequency modes shift to lower energy by as much as 3% (Figure 2b); and 2. the doublets in the spectrum collapse (Figure 3). These changes are tabulated in Table I. Both of the above observations are quite unusual in a qualitative and quantitative sense for a "normal" aromatic $S_1 \leftarrow S_0$ transition.[29] Additionally, the 7AZI spectrum displays a large number of vibronic features of quite weak intensity which are not very obvious from the figures. This is another striking aspect of the 7AZI spectrum.

Upon comparing the 7AZI spectrum with that of indole[18,30], one finds few common features. The vibronic features between 700 to 800 cm^{-1} are similar for both molecules but the doublet structure here and throughout the spectrum (for weaker features) is unique to 7AZI. The low energy peaks at 234, 280, 306, 467, and 483 cm^{-1} are also unique to 7AZI. These differences between the two spectra are surprising considering the $S_1 \leftarrow S_0$ transition is supposed to be to the

same $\pi\pi^*$ ^1L_b S_1 state in both instances. Moreover, indole has only two weak vibronic features below 600 cm^{-1} [18,30], while 7AZI has more than 13 relatively intense low energy features.

The unusually large number of low lying vibronic features for 7AZI and the difference between the 7AZI, d_1-7AZI and indole spectra can be accounted for by two molecular properties of 7AZI: 1. the molecule is nonplanar in S_1, particularly at the N_1-H_{10} pyrrolic site; and 2. strong $n\pi^*$ - $\pi\pi^*$ vibronic mixing occurs in the region of the $S_1 \leftarrow S_0$ transition.

The nonplanarity of 7AZI in the S_1 state (in particular at H_{10}) would account for the large deuterium substitution (shifts and collapse of doublets) effect on the spectrum and might also lead to an increased number of allowed vibronic transitions. Even this nonplanarity, however, should not give rise directly to so many transitions.

We suggest that a strong $n\pi^*$ - $\pi\pi^*$ mixing would account for the apparent density of vibronic transitions in the $S_1 \leftarrow S_0$ manifold. Similar suggestions have been made for isoquinoline[21,31], quinoline[21], 2-hydroxypyridine[22] and other molecules. The intensity of these vibronic transitions comes from the $\pi\pi^*$ state but the peak positions are associated with $n\pi^*$ - $\pi\pi^*$ vibronic resonances and couplings. As in the case of isoquinoline, we are unable to detect direct absorption (through either TOFMS or FE experiments) from S_0 to the $n\pi^*$ excited state.

In order to elucidate this problem further, two approaches are useful: 1. calculation of the S_0 and S_1 geometry; and 2. clustering of 7AZI with various solvents to alter the $n\pi^*$ - $\pi\pi^*$ coupling and perhaps to affect the 7AZI planarity.

B. 7-Azaindole - Calculations

The geometry and atomic point charge distribution for 7AZI in both the ground and first excited singlet states are calculated using MOPAC 5 AM1 and PM3 Hamiltonians. These data are summarized in Tables II and III. The optimum geometries calculated with either Hamiltonian are the same for the ground state, although significant differences are found for the atomic partial charges at various atoms (e.g., C_9 and N_1). For the first excited state, the two Hamiltonians give different geometries: the AM1 Hamiltonian yields a nonplanar molecule (C_9 and H_{10}) while the PM3 Hamiltonian yields a planar molecule. These calculations, however, are neither very accurate

nor reliable as the convergence criteria for optimum S_1 geometry for both these calculations is poor ($\approx$ 7 for S_1 as opposed to 0.01 for S_0). Moreover, different optimum geometries obtain for different initial input geometries. The general trend of results for the AM1 calculations seems sound, however; 7AZI apparently has a propensity for nonplanarity of the pyrrolic ring in S_1, especially at C_9 and H_{10}. The AM1 Hamiltonian can generate a nonplanar 7AZI for the first excited singlet state. H_{10} is typically out of plane by 18-19° (see Figure 4).

We can conclude from both the experimental and theoretical results that some of the spectral crowding and doubling of various vibronic features in the 7AZI spectrum may well be due to the loss of planarity in S_1. The potential well for H_{10} motion with respect to the plane of the heavy atom ring is probably a double well with a large barrier to the zero degree, planar conformation.

C. 7-Azaindole$(Ar)_1$ and $(CH_4)_1$ clusters

The general reason to look at cluster spectra at this point is to resolve the two issues posed above: 1. the (S_1) nonplanarity of 7AZI and its ensuing double well potential surface; and 2. the importance of $n\pi^* - \pi\pi^*$ mixing for this molecule.

Spectra for 7AZI$(Ar)_1$ and $(CH_4)_1$ are presented in Figure 5. The cluster shifts for the 0_0^0 transition are -18 cm^{-1} for 7AZI$(Ar)_1$ and -46 cm^{-1} for 7AZI$(CH_4)_1$. These are quite typical of cluster shifts for other solute systems. For example for toluene, pyrazine, pyrimidine, benzene, and indole the origin shift for 1:1 methane clusters are -43^{12}, -33^{13}, -57^{32}, -41^{11}, and -36^{33} cm^{-1}, respectively and the shifts for benzene and indole with argon are -21^{34} and -26^{35} cm^{-1}, respectively.

Calculations of cluster geometry are presented in Figure 6. Again very typical behavior is observed for the single minimum energy configurations of these clusters.

By contrast, comparison of the vibrational structure of these clusters with each other and bare 7AZI shows substantial changes in the vibronic features brought about by clustering. This is strong evidence that $n\pi^* - \pi\pi^*$ mixing is distorting the observed cluster and bare molecule vibronic structure. Thus the apparent density of vibronic features in the 7AZI bare molecule spectrum may well be due to vibronic coupling between a low lying $n\pi^*$ state and the "observed" $\pi\pi^*$ state, "S_1".

The observed vibronic transitions in this region can reflect this interaction and not existing vibrational structure in the 7AZI excited $\pi\pi^*$ electronic state.

At higher vibrational levels in S_1 the transition intensity of both clusters begins to decrease due to vibrational predissociation of the clusters.[36] The intense feature at +934 cm^{-1} above the 0_0^0 transition of the bare molecule is no longer observed either due to vibrational predissociation or removal of the $n\pi^*$ - $\pi\pi^*$ interaction upon clustering. In either event, this demonstrates that the 934 cm^{-1} feature is a vibronic one and not a new electronic origin (e.g., ^1L_a). Thus the observed spectra are suggested to be due to a transition involving the ^1L_b ($\pi\pi^*$). The excited ^1L_b ($\pi\pi^*$) state probably interacts with a lower energy singlet $n\pi^*$ state to produce the observed complex high density $S_1 \leftarrow S_0$ transition in the 34,600 to 35,600 cm^{-1} region.

D. 7-Azaindole/H_2O Clusters

The spectra of 7AZI$(H_2O)_{1,2,3}$ are presented in Figure 7. The 0_0^0 transition for 7AZI$(H_2O)_1$ is located at 33,346 cm^{-1}, red shifted by 1288 cm^{-1} from the bare molecule 0_0^0 transition. The 7AZI$(H_2O)_{2,3}$ spectra are further red shifted by 1997 cm^{-1} and 2075 cm^{-1}, respectively. These red shifts are enormous considering those found for benzene[32] (+85 cm^{-1}), indole[37] (-135 cm^{-1}), phenol[38] (- 356 cm^{-1}), fluorene[39] (+ 57 cm^{-1}), and isoquinoline[21] (0.6 cm^{-1}) clusters with $(H_2O)_1$. The unusually large red shift for 7AZI/water clusters suggests that the $n\pi^*$ - $\pi\pi^*$ excited state interaction has been (at least partially) removed by the interaction of 7AZI with water. Hydrogen bonding solvents are known to raise the energy of $n\pi^*$ states with respect to $\pi\pi^*$ states.[40] The suggested mechanism for this increase in the $n\pi^*$ excitation energy is the lowering of the ground state n orbital energy due to hydrogen bond formation between water and the lone pair electrons on the ring nitrogen (see Figure 1b). If the $n\pi^*$ state were raised in energy above the $\pi\pi^*$ state, additional lowering in energy of the $\pi\pi^*$ state would occur through interaction between these two zero order descriptions.

Not only is the origin shift of 7AZI/water clusters with respect to 7AZI suggestive of excited electronic state mixing but the observed cluster vibronic structure is as well. Note that the

low energy modes of 7AZI S_1 have changed nearly 33% in 7AZI$(H_2O)_1$: this is almost unique for vdW clusters. Apparent overtone structure is observed for both systems. The strong 7AZI feature at 934 cm^{-1} is missing in 7AZI$(H_2O)_n$ spectra; vibrational predissociation is unlikely to be the reason for this absent feature based on binding energy considerations.

Given the large cluster shifts, the change in S_1 vibrational structure upon clustering with water, and the absence of any other 7AZI/water features in the 33,000 to 36,000 cm^{-1}, we believe that the excited state observed for 7AZI/water is ^1L_b with a significant removal of $n\pi^*$ state interference. The ^1L_a state is probably not observed in this region.

Cluster structure has been explored through a number of different calculations. Both MOPAC 5 and potential energy calculations are performed on the 7AZI$(H_2O)_1$ clusters. Table IV and Figures 8 and 9 summarize the results of such studies. The MOPAC 5 calculation gives distorted double hydrogen bonded structures for the PM3 Hamiltonian (Figure 8a) but single hydrogen bonded structures for the AM1 Hamiltonian (Figure 8b). In neither case are the water or 7AZI structures and charges much different from those of the isolated individual molecules. Note that the MOPAC 5 calculation [tested in this study for the pyrazine[41] and pyrimidine[41] dimers and pyrazine$(NH_3)_1$[32]] tends to underestimate the vdW dispersion interaction between the aromatic π-system and the solvent heavy atom(s). In general these structures do not appear to be very reliable.

The potential energy calculation (Figure 9) generates different structures for 7AZI$(H_2O)_1$ depending on the Hamiltonian employed for the isolated molecule structure calculations. The PM3 molecules generate a single structure while the AM1 molecules yield three different structures, one of which is the PM3 structure. Nevertheless, all of these structures are the basic compromise structure falling between those found for only hydrogen bonding interactions and those found for only dispersion interactions. If a double hydrogen bonded structure (Figure 8a) is fixed for the potential energy calculation as an initial geometry, a binding energy of ca. 560 cm^{-1} obtains; this structure is, however, not at a minimum on the potential surface. Such minimum energy structures are presented in Figure 9. This of course makes a good deal of "intuitive sense". We believe that

these geometries are more reliable than either the PM3 or AM1 MOPAC 5 cluster/dimer geometries (Figure 8).

Potential energy calculations for higher order clusters, based on PM3 molecules, generate two significant results: a plethora of structures, and, if the ring center positions are occupied, a double hydrogen bonded cyclic structure. The suggestion here is that the largest interaction between 7AZI and water is at the π-system of 7AZI, but that once these positions are occupied the hydrogen bonding structures (cyclic and otherwise) can be realized.

E. 7-Azaindole/D_2O Clusters

If D_2O is substituted for H_2O in the expansion system mixture, mass resolved excitation spectra are observed for 7AZI (118 amu), (118 + 1) amu, (118 + 18) amu, (118 + 19) amu, (118 + 20) amu, and (118 + 21) amu, etc. The spectra at mass channels (118 + 1) and (118 + 18) amu are identical to those of d_1 - 7AZI and 7AZI$(H_2O)_1$, respectively. Spectra taken at mass channel (118 + 18), (118 + 19), (118 + 20) and (118 + 21) amu are presented in Figure 10. The spectra certainly suggest that a rapid exchange between the acidic H_{10} of 7AZI and the protons of water takes place on the S_0 potential surface. Thus the spectrum of Figure 10b is composed of d_1 - 7AZI$(H_2O)_1$ and 7AZI$(HOD)_1$ spectra and the spectrum of Figure 10c is composed of d_1 - 7AZI$(HOD)_1$ and 7AZI$(D_2O)_1$ spectra. The spectrum taken at mass channel (118 + 21) amu (Figure 10d) is then due to d_1 - 7AZI$(D_2O)_1$. The ratio of peak heights in these spectra is roughly that expected for the statistical distribution of the various isotopic cluster species.

Two features of Figure 10 are worth special emphasis. First, both spectra at (118 + 19) amu and (118 + 20) amu consist of three origin transition: three origins, of course, implies the existence of three distinct sites for the deuterium substitution. The three sites are most likely H_{10} of 7AZI (as found specifically for this particular deuteration) and the two distinct proton sites on the water molecule in the cluster. This experimental observation is not consistent with the AM1 MOPAC 5 geometry depicted in Figure 8b. Second, the spectrum of d_1 - 7AZI$(D_2O)_1$ is much simpler (fewer transitions) than that of 7AZI$(H_2O)_1$ (compare Figures 10a and 10d). The $n\pi^*$ - $\pi\pi^*$ interaction suggested above for 7AZI may thus not be totally removed even in the presence of

water solvation. This is perhaps further evidence against a strong hydrogen bonded cyclic structure for 7AZI$(H_2O)_1$ as generated by the PM3 MOPAC 5 cluster calculation (Figure 8a).

Figure 11 shows the spectrum taken at mass channel (118+37). The mass corresponds to 7AZI plus two waters with one of the water hydrogens or H_{10} is dueterated. The five possible conformers due to the different dueterium substitution sites appear in three distinctive bands of electronic origins. The band B apparently represents a single peak and can be tentatively assigned to d_1-7AZI$(H_2O)_2$, while each of bands A and C is apparently composed of two very close peaks and can tentatively be assigned to 7AZI(H_2O)(DOH). Attempts to identify the structure of 7AZI plus two waters from Figure 11 meet with some difficulty; however, we believe that , if the double hydrogen bonding structure in Figure 8a were realistic, four distinctive bands would be observed at mass channel (118+37) for the cluster origin.

F. 7-Azaindole/Alcohol Clusters

Figure 12 shows the 2-color TOFMS of 7AZI$(CH_3OH)_1$ and 7AZI$(C_2H_5OH)_1$. 7AZI$(CH_3OH)_1$ displays a single origin while 7AZI$(C_2H_5OH)_1$ shows multiple origins. The spectra do not display common vibronic features, again suggesting that the $n\pi^* - \pi\pi^*$ interaction has not been removed in these clusters.

The potential energy calculations for 7AZI$(CH_3OH)_1$ are presented in Figure 13. Two structures are found for this system. The hydrogen bonding interaction weakens for ROH compared to HOH and the electron density of R is far greater than that of H; the dispersion interaction between the solvent electron density and the ring π-system becomes more significant in these instances. The ethanol cluster has many different calculated conformations due mostly to orientations of the ethyl group: basically the cluster geometry for 7AZI$(CH_3OH)_1$ and $(C_2H_5OH)_1$ clusters are similar.

G. 7-Azaindole/Ammonia Clusters

7AZI clustered with ammonia has a spectrum different from both the bare molecule 7AZI and the other clusters, as presented in Figure 14. Note especially the low lying vdW modes following within 50 cm^{-1} of the 0_0^0 transition and the low lying molecular vibronic features at

ca. 200 and 400 cm^{-1}. The 7AZI$(NH_3)_1$ spectrum looks much simpler (i.e., has fewer transitions) than the 7AZI$(H_2O)_1$ spectrum.

According to the potential energy calculation, the NH_3 molecule coordinates to the aromatic π - system for the minimum energy configuration (See Figure 15). The 7AZI$(NH_3)_2$ cluster has the typical symmetric and asymmetric structures as depicted in Figure 15. The observed spectrum for 7AZI$(NH_3)_2$ is thought to arise from the symmetric structure because of the cluster shift, the large number (five) of different asymmetric structures generated in the calculation, and the fact that 80% of the calculated minimum energy structures are of the form displayed in Figure 15b.

H. van der Waals Modes for the 7AZI Clusters

Figure 16 summarizes the vdW mode spectra for the various clusters. Note that in general the intensity of these features is weak and the Franck-Condon envelop for the transition has its maximum at the $\Delta v = 0$ position. Similar results are obtained for most vdW clusters.[31] None of the features above 0_0^0+ 100 cm^{-1} in the various clusters can be attributed to vdW modes.

I. Cluster Shifts

Cluster red shifts are large and probably more indicative of the $n\pi^*$-$\pi\pi^*$ residual mixing in the cluster than they are of solute/solvent interaction energy. For example, the shifts presented in Table V do not reflect hydrogen bonding strengths. Moreover, the addition of a second solvent molecule also generates a large red shift in the disolvate cluster. Both observations seem to suggest that a planar double hydrogen bonded structure is not the lowest energy structure for these solute/solvent systems in the gas phase.

V. SUMMARY AND CONCLUSIONS

Results of these studies for 7AZI and its clusters with argon, methane, water, alcohols, and ammonia can be summarized as follows: 1. the spectrum of the bare molecule is quite congested with many low energy vibronic features and apparent doublets appearing in the mass resolved excitation spectrum; 2. the cluster spectra are also of the same nature but the vibronic structure is quite different for each particular cluster; 3. the vibronic doublets disappear upon deuteration of 7AZI at H_{10}; 4. calculations suggest that 7AZI may be nonplanar in S_1; 5. potential energy

calculations suggest that cyclic hydrogen bonding between water, alcohols and ammonia and 7AZI is not a stable low energy structure for the first two solvent molecules in the cluster; and 6. all cluster spectra are red shifted from the bare molecule origin, especially for polar solvents as indicated in Table V.

The conclusions we draw from these results are as follows: 1. strong $n\pi^* - \pi\pi^*$ vibronic mixing occurs between the ^1L_b $\pi\pi^*$ excited state and a lower lying $n\pi^*$ state; 2. this vibronic mixing is only partially removed by clustering; 3. a cyclic hydrogen bonded structure is not achieved for the $7AZI(H_2O)_{1,2}$ $7AZI(ROH)_{1,2}$, or $7AZI(NH_3)_{1,2}$ clusters; and 4. the 7AZI molecule is nonplanar (at H_{10} - N_1 on the pyrrole ring) in the first excited singlet state.

The large spectral $S_1 \leftarrow S_0$ red shifts for water, alcohol, and ammonia 7AZI clusters do not necessarily imply a cyclic hydrogen bonded cluster structure because the (supposed) stability of these structures would not correlate with size of the red shift.

Finally, these results suggest that the double hydrogen bonding structures assumed to be intermediates in the 7AZI tautomerization process in condensed phases may only be present in rather high solvent density systems for which solvent molecules occupy the ring centered solvation sites of 7AZI. Under such conditions, solvent molecules may occupy the lower binding energy hydrogen bonded sites at the N_7 and N_1-H_{10} positions (See Figure 1a).

ACKNOWLEDGMENT

This work is supported in part by grants from NSF and ONR. We wish to thank Professor J. M. Hollas for helpful communications on 7-AZI spectroscopy and for discussion of some of his unpublished results on 7-AZI.

Reference

1. C.A. Taylor, M.A. El-Bayoumi and M. Kasha, Proc. Natn. Acad. Sci. U.S.A **63**, 253 (1969).
2. K.C. Ingham and M.A. El-Bayoumi, J. Am. Chem. Soc. **96**,1674 (1974).
3. P. Stäglich and M. Zander, Z. Naturforsh. **31a**, 1391 (1976).
4. K. Tokumura, Y. Watanabe and M. Itoh, J. Phys. Chem. **90**, 2362 (1986). K. Tokumura, Y. Watanabe, M. Udagawa and M. Itoh, J. Am. Chem. Soc.**109**, 1346 (1987).
5. H. Bulska and A. Chodkowsks, J. Am. Chem. Soc. **80**, 3259 (1980).
6. W.M. Hetherington III, R.M. Micheels and K.B. Eisenthal, Chem. Phys. Lett. **66**, 230 (1979).
7. D. McMorrow and T.J. Aartsma, Chem. Phys. Lett. **125**, 581 (1986).
8. R.S. Moog, S.C. Bovino and J.C. Simon, J. Phys. Chem. **92**, 6545 (1988).
9. C. R. Cantor and P.R. Schimmel, Biophysical Chemistry I, (Freedman, 1980).
10. R. Nowak, J.A. Menapace and E.R. Bernstein, J. Chem. Phys. **89**, 1309 (1988).
11. M. Schauer and E.R. Bernstein, J. Chem. Phys. **82**, 726 (1985).
12. M. Schauer, K. S. Law and E.R. Bernstein, J. Chem. Phys. **82**, 736 (1985).
13. J. Wanna and E.R. Bernstein, J. Chem. Phys. **84**, 927 (1986).
14. K. Fuke and K. Kaya, J. Phys. Chem. **93**, 614 (1989).
15. K. Fuke, H. Yoshiuchi and K. Kaya, J. Phys. chem. **88**, 5840 (1984).
16. T.P. Ruane, thesis, Princeton University (1987).
17. J. Catalan and P. Perez, J. Theor. Biol. **81**, 213 (1979).
18. R. Bersohn, U. Even and J. Jortner, J. Chem. Phys. **80**, 1050 (1984).
19. R.W. Wagner, thesis, Michigan State University (1971).
20. L.B. Clark and L. Tinoco, J. Am. Chem. Soc. **87**, 11 (1965).
21. J. Wanna and E.R. Bernstein, J. Chem Phys. **86**, 6707 (1987).
22. M.R. Nimlos, D.F. Kelley and E.R. Bernstein, J. Phys Chem. **93**, 643 (1989).
23. P. Bryant and J.M. Hollas, Indian J. Phys. **60B**,1 (1986).
24. E.R. Bernstein, K. Law and M. Schauer, J. Chem. Phys. **80**, 207 (1984).
25. J. J. P. Stewart, MOPAC. A General Molecular Orbital Package, 5th ed., (1988).

26. M.J.S. Dewar, E.G. Zoebisch, E.F. Healy and J.J.P. Stewart, J. Am. Chem. Soc. **107**, 3902 (1985).

27. J. J.P. Stewart, J. Compt. Chem. **10**, 209, 221 (1989).

28. G. Nemethy, M.S. Pottle and H.A. Scherga, J. Phys. Chem. **87**, 188 (1983). F.A. Momany, L.M. Carruthers, R.F. McGuire and H.A. Scherga, J. Phys. Chem. **78**, 1595 (1974).

29. Atomic and Molecular Clusters, E.R. Bernstein, ed., (Elsevier, 1989).

30. J. Hager and S.C. Wallace, J. Phys. Chem. **87**, 2121 (1983).

31. A. Hiraya, Y. Achiba, K. Kimura and E.C. Lim, J. Chem. Phys. **81**, 3345 (1984).

32. J. Wanna, J.A. Menapace and E.R. Bernstein, J. Chem. Phys. **85**, 1795 (1986).

33. J. Hager, M. Ivanco, M.A. Smith and S.C. Wallace, Chem. Phys. Lett. **113**, 503 (1985).

34. T.A. Stephenson and S.A. Rice, J. Chem. Phys. **81**, 1083 (1984).

35. J. Hager and S.C. Wallace, J. Phys. Chem. **88**, 5513 (1984).

36. D.F. Kelley and E.R. Bernstein, J. Phys. Chem. **90**, 5164 (1986).

37. T. Montoro, C. Jourvet, A.L. Campillo and B. Soep, J. Phys. Chem. **87**, 3582 (1983).

38. K. Fuke and K. Kaya, Chem. Phys. Lett. **94**, 97 (1983).

39. H.S. Im, V.H. Grassian and E.R. Bernstein, J. Phys. Chem. (1989), to be published.

40. See ref. 21 and references quoted therein.

41. J. Wanna, J.A. Menapace and E.R. Bernstein, J. Chem. Phys. **85**, 777 (1986).

Table I

Deuterium substitution (H_{10}, see Figure 1) effect on vibrational energies of 7AZI. (Not all weak peaks after 700 cm^{-1} are tabulated.)

Vibrational energies (cm^{-1})		Intensity
7AZI	d_1-7AZI	
0(34634)	0(34637)	vs, 0_0^0 origin
234	230	m
280	272	s
306	301	m
372	366	w
404, 409	397, 400	w
457	453	w
467	458	m
483	475	s
527	523	w
547	545	w
574, 578	567, 573	w
672	652	w
682	688	w
696	695	w
706	700	w
714, 718	708, 709	m
730, 735	725, 726	s
747	735, 736	m
757	742, 743	s
772	750,752	w
796		m
857, 866	851, 859	w
934	934	s

Table II

Optimum geometry and charge distribution for 7AZI in the ground state. Results from MOPAC5 calculations using the PM3 and AM1 Hamiltonians.

Atom[a] I	Bond length (Å) PM3	AM1	Bond Angle (degrees) PM3	AM1	Twist Angle (degrees) PM3	AM1	J K L[b]	Charge (e) PM3	AM1
1 N								0.3155	-0.2033
2C	1.410	1.397					1	-0.2419	-0.0762
3 C	1.381	1.392	109.27	110.59			2 1	-0.1466	-0.1921
4 C	1.403	1.396	134.72	135.68	-179.93	180.00	9 3 2	-0.0035	-0.0420
5 C	1.378	1.386	117.62	117.99	179.98	180.00	4 9 3	-0.1871	-0.2116
6 C	1.417	1.419	120.96	119.86	0.01	0.03	5 4 9	-0.0454	-0.0530
7 N	1.337	1.336	123.17	125.34	-0.02	-0.02	6 5 4	-0.0687	-0.1454
8 C	1.402	1.402	107.95	108.14	0.15	0.09	1 2 3	-0.1681	0.0281
9 C	1.424	1.459	107.87	107.59	0.12	-0.07	8 1 2	-0.1300	-0.1210
10 H	0.987	0.985	125.66	126.46	179.55	179.87	1 2 3	0.0768	0.2592
11 H	1.090	1.092	128.40	129.33	179.98	179.98	2 3 9	0.1400	0.1676
12 H	1.087	1.085	126.77	126.79	179.91	179.96	3 2 1	0.1285	0.1587
13 H	1.094	1.099	120.50	120.58	180.01	179.99	4 9 8	0.1061	0.1386
14 H	1.094	1.097	120.43	120.95	180.00	180.02	5 4 9	0.1118	0.1407
15 H	1.096	1.106	121.34	119.75	179.99	179.99	6 5 4	0.1125	0.1568

Final heat of formation: 48.15 kCal/mol for PM3
66.97 kCal/mol for AM1

Footnotes:

a: Numbering of atoms are as specified in Figure 1a.

b: The bond length is defined between I and J.
The bond angle is defined between lines (IJ) and (JK).
The twisting angle is defined between plane(JKL) and line (IJ).

Table III

Optimum geometry and charge distribution for 7AZI in the first excited singlet state. Results from MOPAC5 calculations using the PM3 and AM1 Hamiltonians.

Atom I	Bond length (Å) PM3	AM1	Bond Angle (degrees) PM3	AM1	Twist Angle (degrees) PM3	AM1	J	K	L	Charge (e) PM3	AM1
1N										0.4769	-0.1686
2C	1.364	1.362					1			-0.4079	-0.1737
3C	1.436	1.459	108.34	110.04			2	1		-0.0031	-0.0743
4C	1.385	1.404	134.98	134.96	-179.80	179.85	9	3	2	-0.1176	-0.1329
5C	1.418	1.404	117.18	116.89	179.82	-179.88	4	9	3	-0.1255	-0.1619
6C	1.377	1.395	121.63	120.82	0.08	1.22	5	4	9	-0.0854	-0.0926
7N	1.395	1.365	122.88	125.20	0.01	-0.42	6	5	4	-0.1268	-0.1743
8C	1.422	1.446	109.76	108.23	-0.18	-3.57	1	2	3	-0.1590	0.0887
9C	1.422	1.454	107.31	107.23	0.20	4.20	8	1	2	-0.1307	-0.1330
10H	0.986	0.993	125.28	126.47	179.86	-161.22	1	2	3	0.0648	0.2510
11H	1.092	1.092	126.66	127.26	179.95	-176.44	2	3	9	0.1585	0.1760
12H	1.088	1.085	125.65	125.26	179.95	-177.45	3	2	1	0.1252	0.1630
13H	1.092	1.095	121.73	121.37	179.93	177.86	4	9	8	0.1111	0.1393
14H	1.094	1.099	118.59	119.66	180.03	-178.98	5	4	9	0.1047	0.1267
15H	1.094	1.105	123.41	121.08	180.02	-178.85	6	5	4	0.1147	0.1562

Final Heat of Formation: 145.81 kCal/mol for PM3
170.05 kCal/mol for AM1

Table IU

Optimum geometry and charge distribution for 7AZI(H_2O)$_1$ in the ground state. Results from MOPAC5 calculations using the PM3 and AM1 Hamiltonians.

Atom I	Bond length (Å)		Bond Angle (degrees)		Twist Angle (degrees)		J	K	L	Charge (e)	
1 N										0.3152	-0.2024
2 C	1.409	1.394					1			-0.2368	-0.0710
3 C	1.381	1.392	109.35	110.57			2	1		-0.1505	-0.1988
4 C	1.398	1.396	134.82	135.89	-179.70	179.94	9	3	2	0.0014	-0.0441
5 C	1.379	1.387	117.63	118.01	-179.86	-179.89	4	9	3	0.1900	-0.2133
6 C	1.416	1.418	120.96	119.89	0.09	0.03	5	4	9	-0.0428	-0.0517
7 N	1.338	1.336	123.22	125.30	-0.05	0.00	6	5	4	-0.0882	-0.1728
8 C	1.402	1.402	107.88	108.04	0.63	0.01	1	2	3	-0.1692	0.0232
9 C	1.427	1.460	108.05	107.71	-0.30	0.02	8	1	2	-0.1299	-0.1189
10 H	0.989	0.993	125.90	126.89	179.34	-179.90	1	2	3	0.0930	0.2809
11 H	1.090	1.092	128.40	129.26	179.98	180.00	2	3	9	0.1410	0.1692
12 H	1.087	1.085	126.80	126.81	179.80	180.03	3	2	1	0.1288	0.1586
13 H	1.094	1.099	120.52	120.59	179.97	180.01	4	9	8	0.1064	0.1391
14 H	1.094	1.097	120.45	120.95	180.02	179.98	5	4	9	0.1124	0.1409
15 H	1.096	1.106	121.28	119.68	179.89	180.00	6	5	4	0.1105	0.1540
16 O	3.352	3.083	150.22	156.81	-174.78	179.76	7	6	5	-0.3851	-0.4082
17 H	0.953	0.962	33.93	66.66	-44.12	-61.76	16	7	6	0.2002	0.2075
18 H	0.951	0.962	107.61	103.36	-86.61	-49.24	16	17	7	0.1835	0.2075

Final heat of formation: -7.71 kCal/mol for PM3
1.04 kCal/mol for AM1

Table U

Solvent shifts for 0_0^0 electronic transition energy of 7AZI

System	Cluster shift (cm^{-1})	Cluster binding energy[a] (cm^{-1})
7AZI	0	–
7AZI(Ar)1	-18	-345
7AZI(CH_4)1	-46	-645
7AZI(H_2O)1	-1288	-819
7AZI(H_2O)2	-1997	-1630, -2760, -2900
7AZI(H_2O)3	-2075	-3500 ~ -4500
7AZI(CH_3OH)1	-1425	-1000, -1100
7AZI(CH_3OH)2	-2376[b]	
7AZI(C_2H_5OH)1	-1454,-1420,-1430	-1000 ~ -1200
7AZI(NH_3)1	-1217	-930
7AZI(NH_3)2	-1694	-1850, -1950
(7AZI)2 [c]	-2342	-2310

a: based on PM3 Hamitonian to optimize 7AZI charges and geometry.

b: reference 16.

c: not shown in this paper.

Figure Captions

Figure 1: The structures of (a) 7AZI (b) 7AZI/water cluster with a double hydrogen bonding structure and (c) $(7AZI)_2$ and its possible tautomerization. The numbering on atoms in a) is used in describing atoms in text and in Tables II, III, IV.

Figure 2: 1-color TOFMS of a) 7AZI and b) d_1-7AZI (H_{10}) for the region 0_0^0 +1000 cm^{-1}. The peak at 34634 cm^{-1} is assigned as the 7AZI origin. The origin features is 2 or 3 times larger than shown.

Figure 3: 1-color TOFMS of a) 7AZI and b) d_1-7AZI with an expanded energy scale. Note the collapse of 7AZI doublet structure in this region upon H_{10} dueteration.

Figure 4: MOPAC 5 result for the first excited singlet state geometry of 7AZI employing the AM1 Hamiltonian.

Figure 5: 2-color TOFMS of a) $7AZI(CH_4)_1$ and (b) $7AZI(Ar)_1$. Wavelength for the ionizing laser is 3200 Å.

Figure 6: Optimum geometries for $7AZI(Ar)_1$ and $7AZI(CH_4)_1$ obtained with a potential energy calculation. Both PM3 and AM1 7AZI structures and charges result in identical cluster geometries. Also shown are cluster binding energies.

Figure 7: 1-color TOFMS of a) $7AZI(H_2O)_1$ and (b) $7AZI(H_2O)_2$. The peaks between 33200 cm^{-1} and 33400 cm^{-1} are 2-3 times larger than shown.

Figure 8: MOPAC 5 results for the local hydrogen bonding structure of $7AZI(H_2O)_1$ using (a) PM3 and (b) AM1 Hamiltonians.

Figure 9: The potential energy calculation results for $7AZI(H_2O)_1$using (a) PM3 molecular structures and charges and (b) AM1 structures and charges. The percentages listed in the figure refer to the number of times each structure is found starting from random initial molecular positions and orientations. Also shown are the cluster binding energies and the percentages of the outcomes.

Figure 10: 1-color TOFMS of 7AZI clustered with D_2O. Detection mass channels are indicated in each spectrum.

Figure 11: 1-color TOFMS of 7AZI clustered with D_2O, detected at mass channel (118+37). (See text for a discussion of the doublet (A, C) and singlet features.)

Figure 12: 2-color TOFMS of a) $7AZI(CH_3OH)_1$ and b) $7AZI(C_2H_5OH)_1$. Wavelength of the ionizing laser is 3225 Å.

Figure 13: The potential energy calculation result for the geometry of $7AZI(CH_3OH)_1$. PM3 molecules are used.

Figure 14: 2-color TOFMS of a) $7AZI(NH_3)_1$ and b) $7AZI(NH_3)_2$. Wavelength of the ionizing laser is 3244 Å.

Figure 15: The potential energy calculation results (based on PM3 molecules) for (a) 7AZI$(NH_3)_1$ and (b) 7AZI$(NH_3)_2$.

Figure 16: Comparison of the vdW modes built on the origins of various clusters. (a) 7AZI, (b) 7AZI$(CH_3OH)_1$, (c) 7AZI$(Ar)_1$, (d) 7AZI$(CH_4)_1$, (e) 7AZI$(H_2O)_1$, (f) 7AZI$(H_2O)_2$, (g) 7AZI$(H_2O)_3$, (h) 7AZI$(NH_3)_1$, (i) 7AZI$(NH_3)_2$.

a

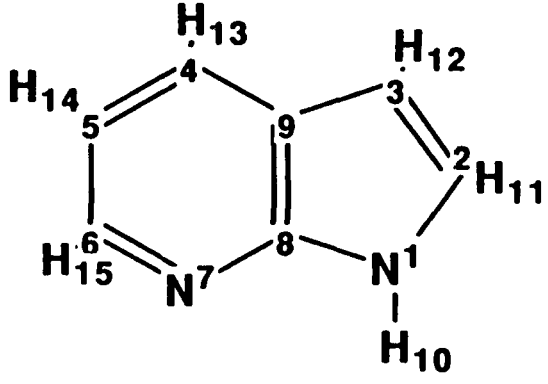

b

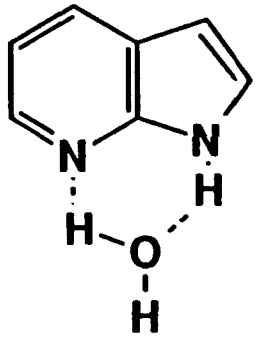

c

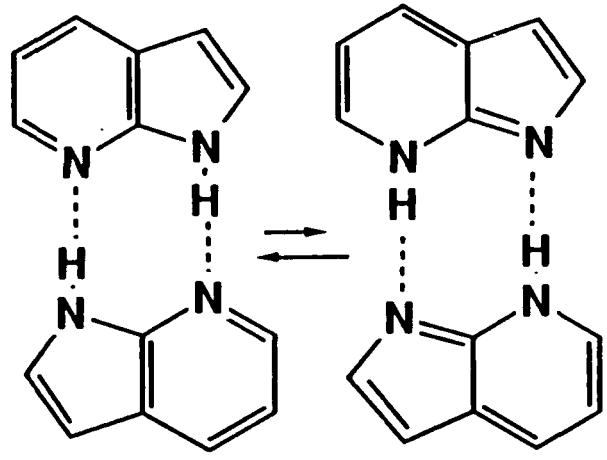

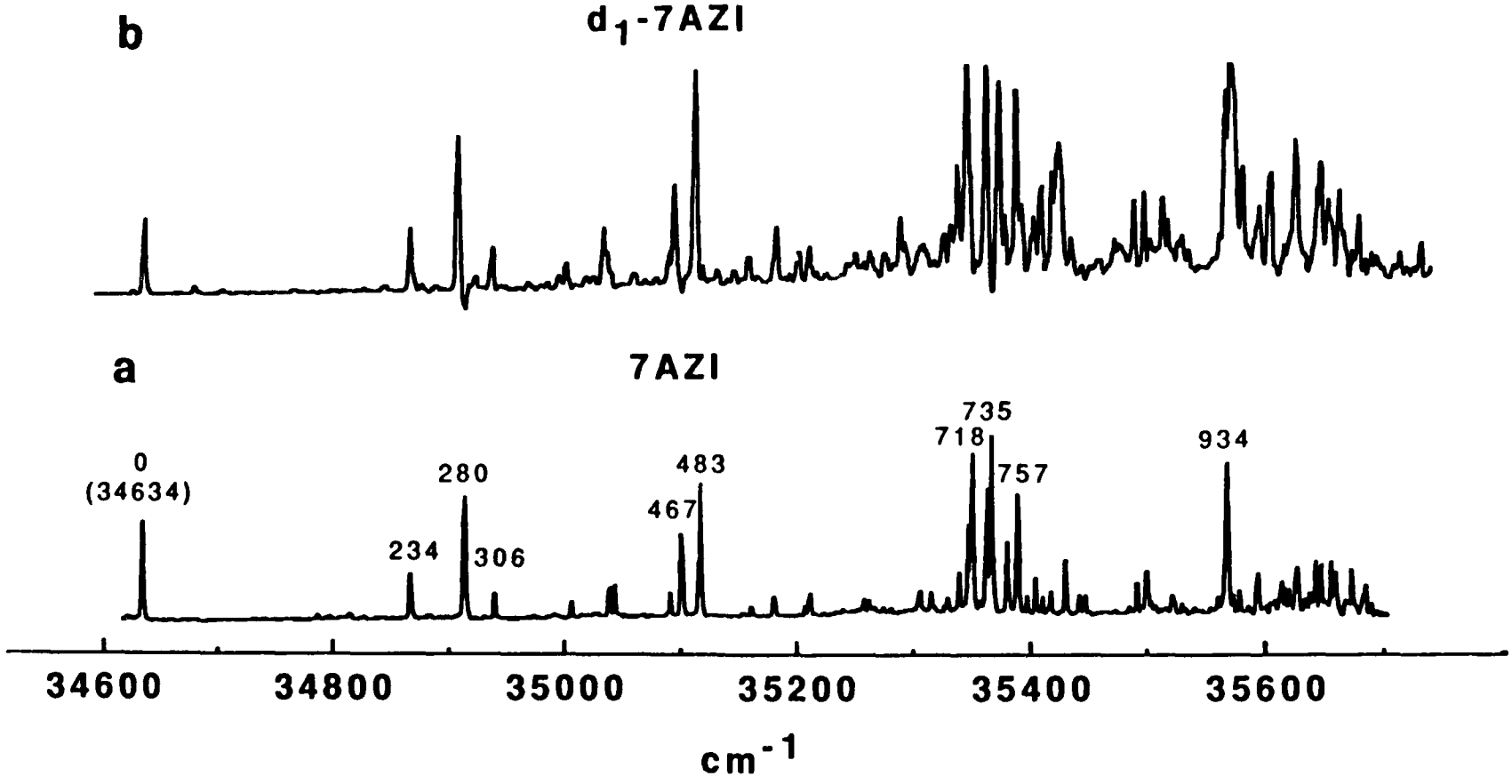
b
d_1-7AZI
a
7AZI
0
(34634)
234
280
306
467
483
718
735
757
934
34600
34800
35000
35200
35400
35600
cm^{-1}

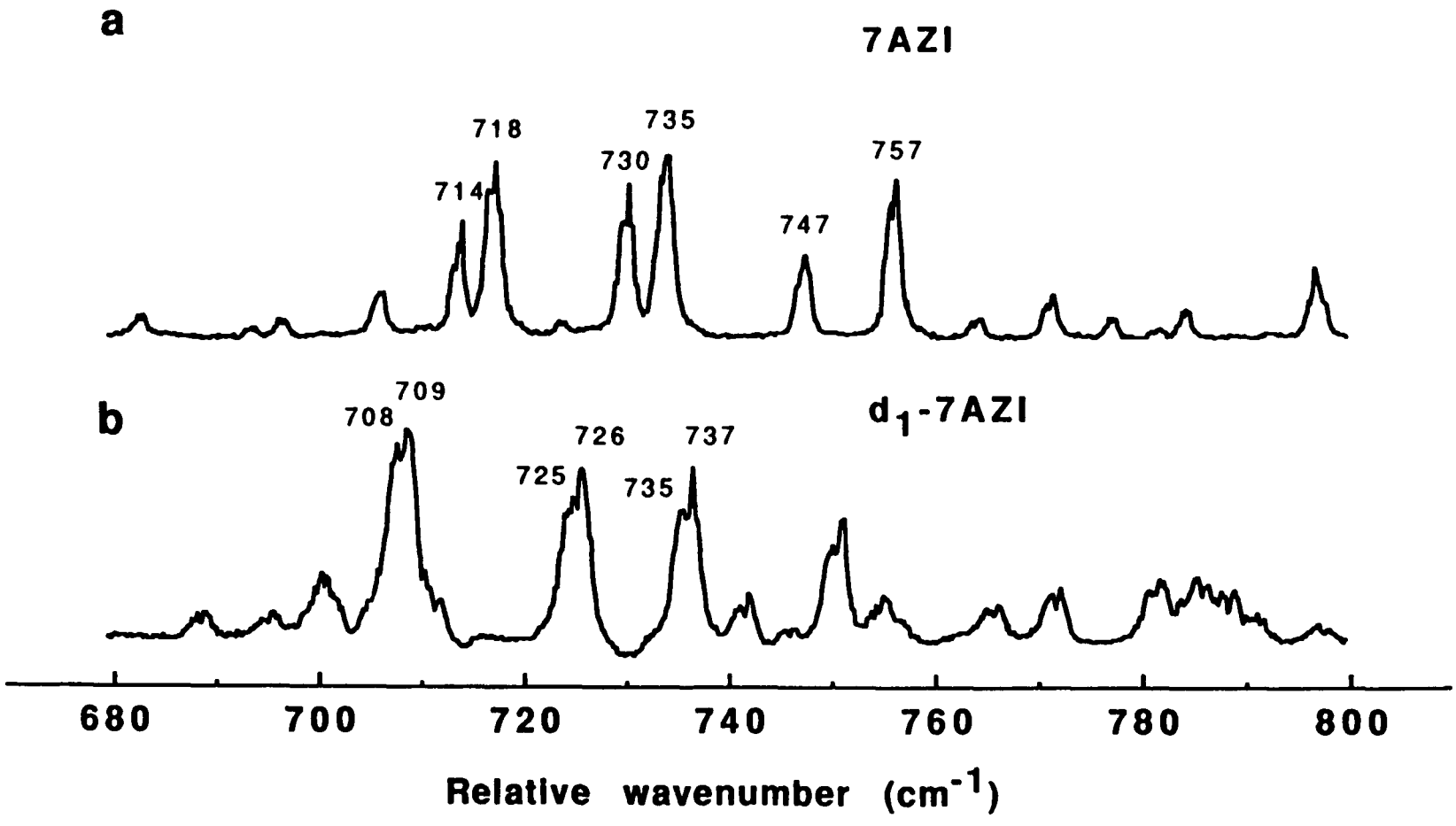
a
7AZI
718
735
730
757
714
747
b
709
708
726
737
725
735
d1-7AZI
680
700
720
740
760
780
800
Relative wavenumber (cm-1)

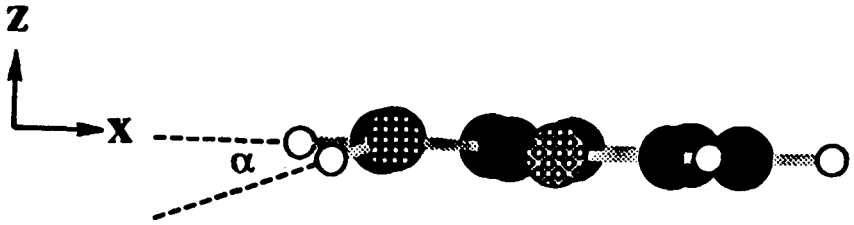

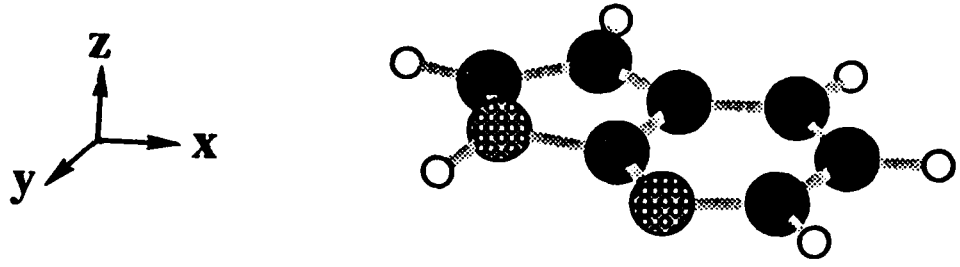

$\alpha = 18.8^{o}$

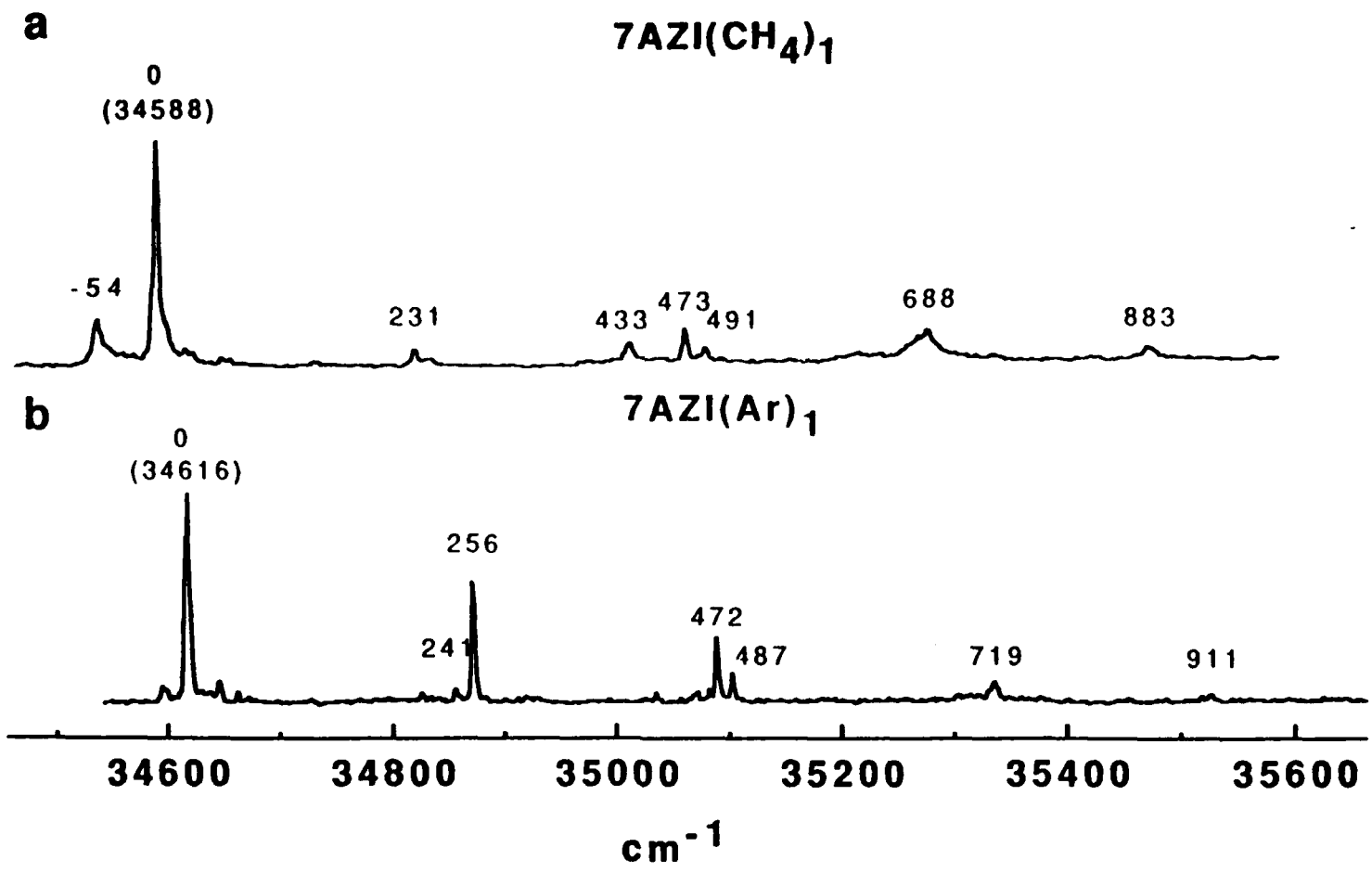
a
7AZI(CH4)1
0
(34588)
-54
231
433
473
491
688
883
b
7AZI(Ar)1
0
(34616)
256
241
472
487
719
911
34600
34800
35000
35200
35400
35600
cm-1

a

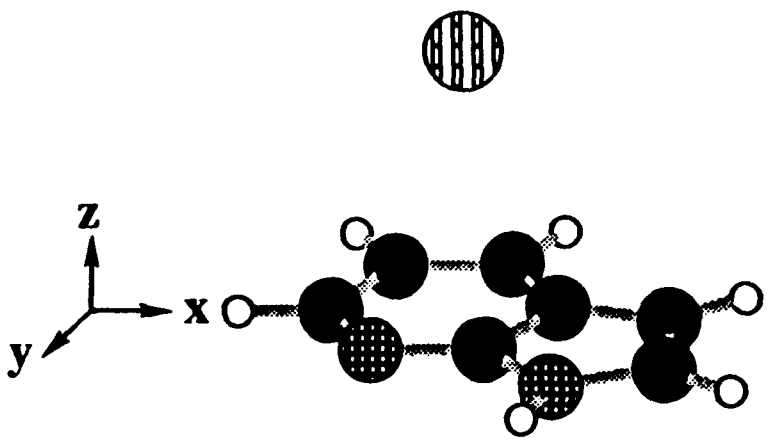

-345 cm-1

b

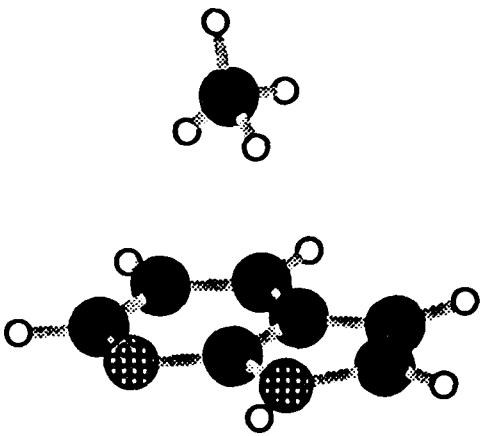

-645 cm-1

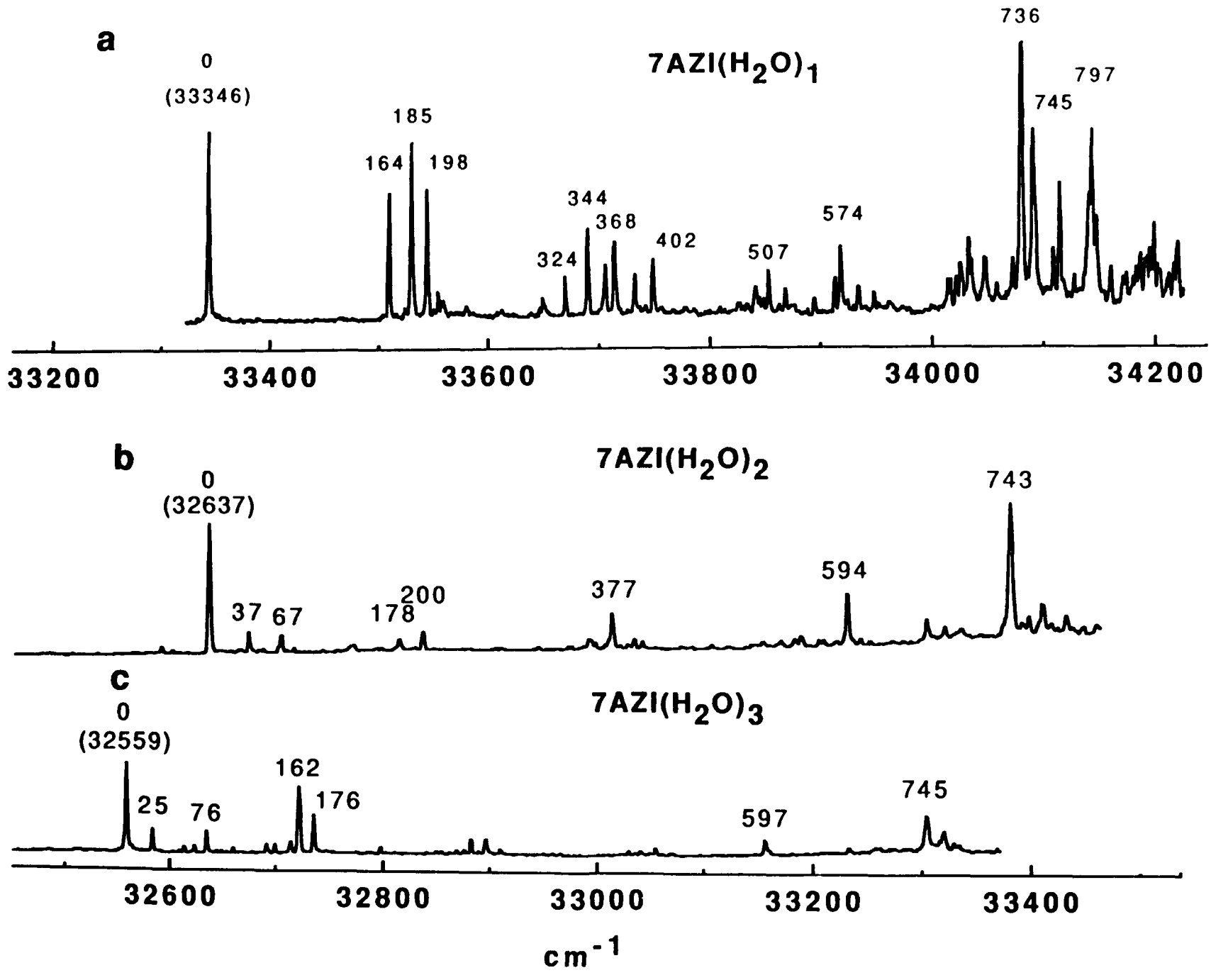
a
0
(33346)
185
164
198
344
368
324
402
507
574
736
745
797
7AZI(H2O)1
33200
33400
33600
33800
34000
34200
b
0
(32637)
37
67
178
200
377
594
743
7AZI(H2O)2
c
0
(32559)
25
76
162
176
597
745
7AZI(H2O)3
32600
32800
33000
33200
33400
cm-1

a PM3

b AM1

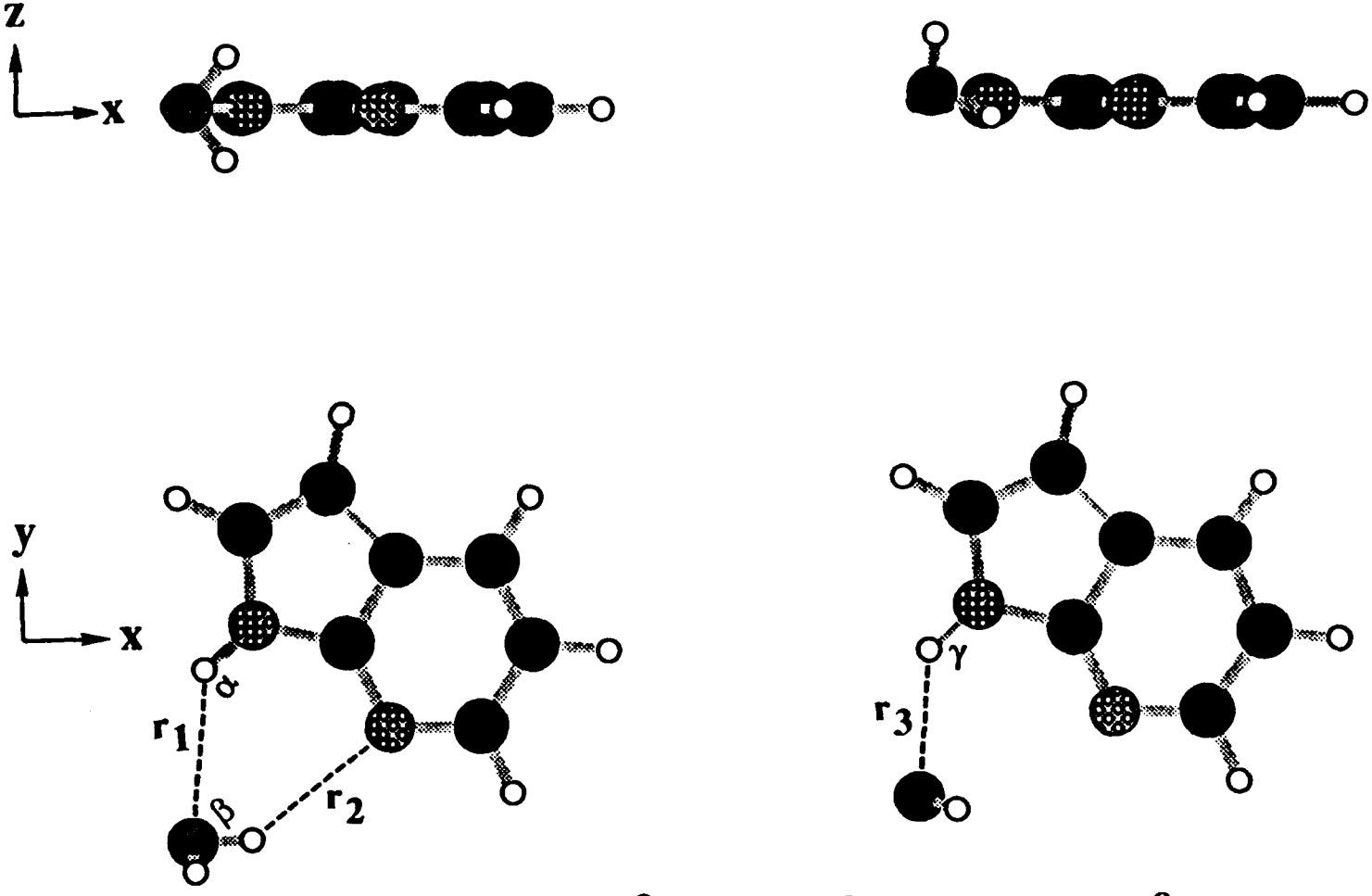

$\alpha = 136.1^{o}$ $\beta = 83.8^{o}$ $\gamma = 135.8^{o}$

$r_1 = 2.542$ Å $r_2 = 2.614$ Å $r_3 = 2.211$ Å

a

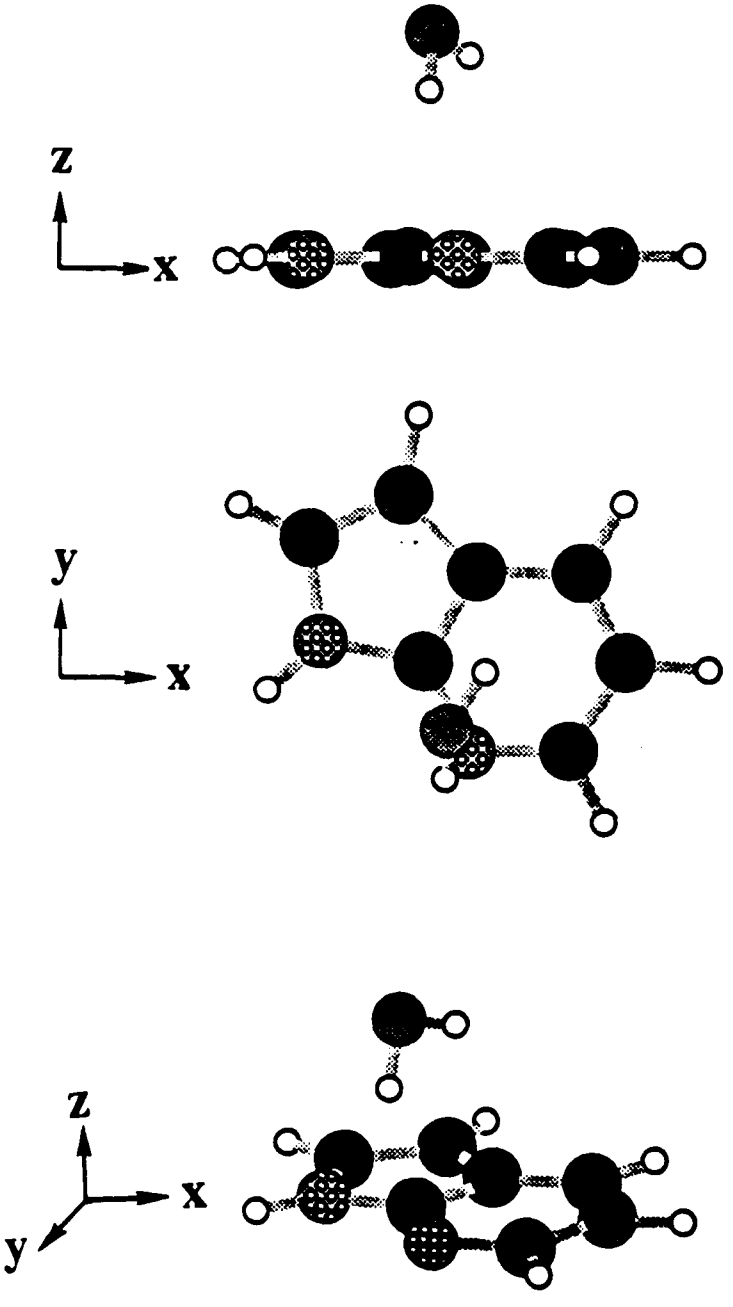

PM3 (100%) -819 cm^{-1}

AM1 (25%) -856 cm^{-1}

b

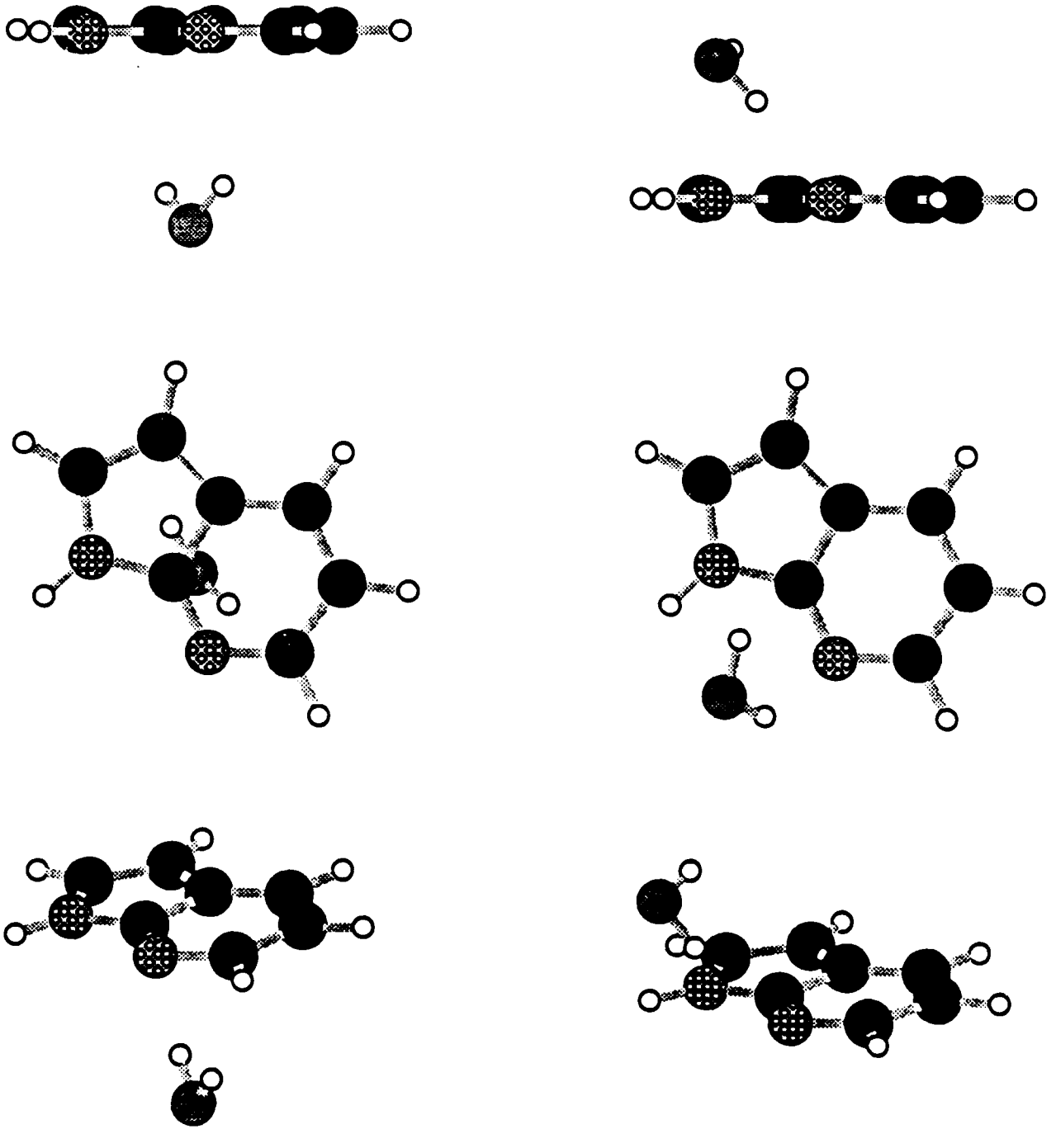

AM1 (36%) -816 cm-1

AM1 (25%) -858 cm-1

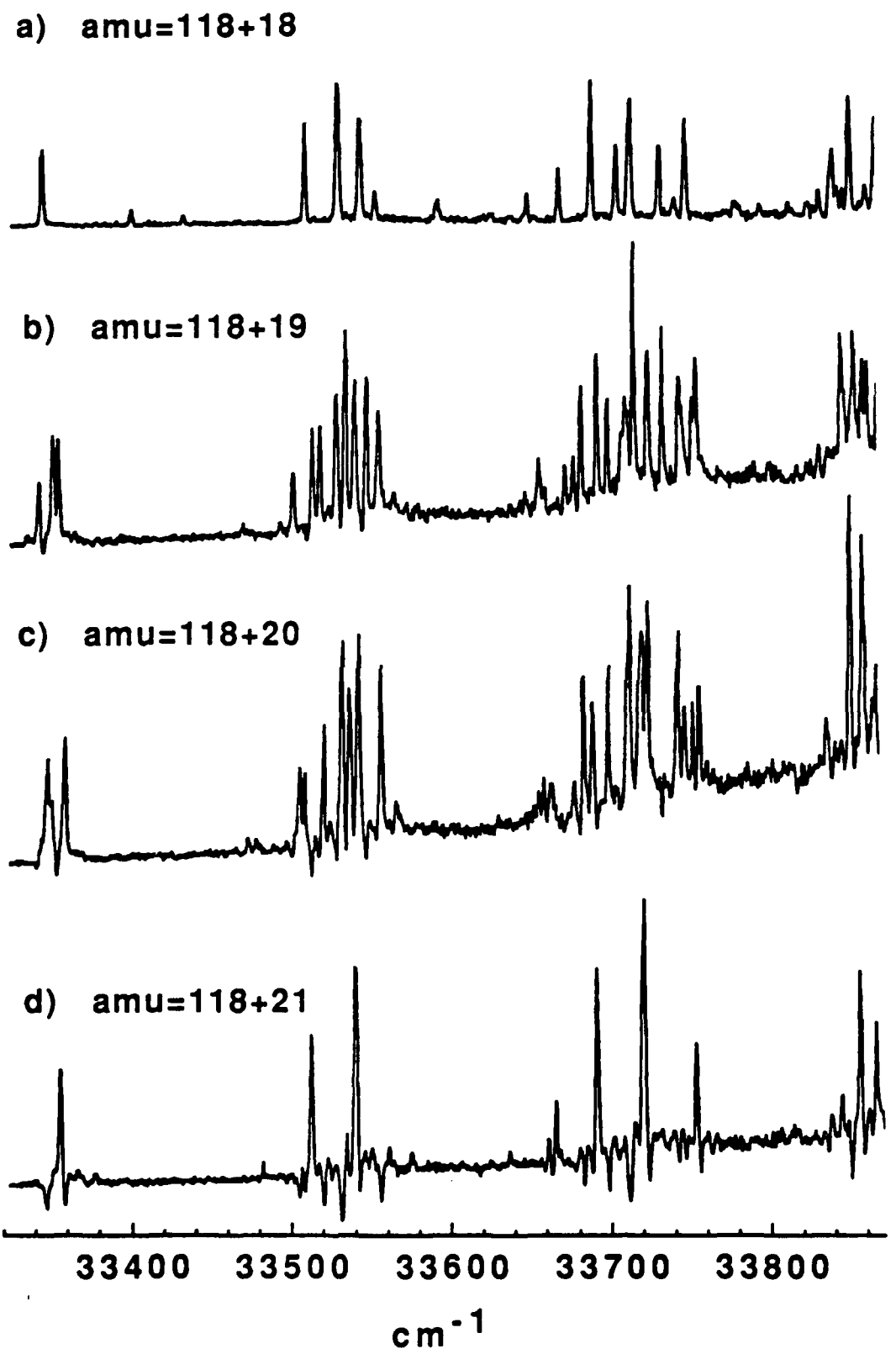
a) amu=118+18
b) amu=118+19
c) amu=118+20
d) amu=118+21
33400
33500
33600
33700
33800
cm-1

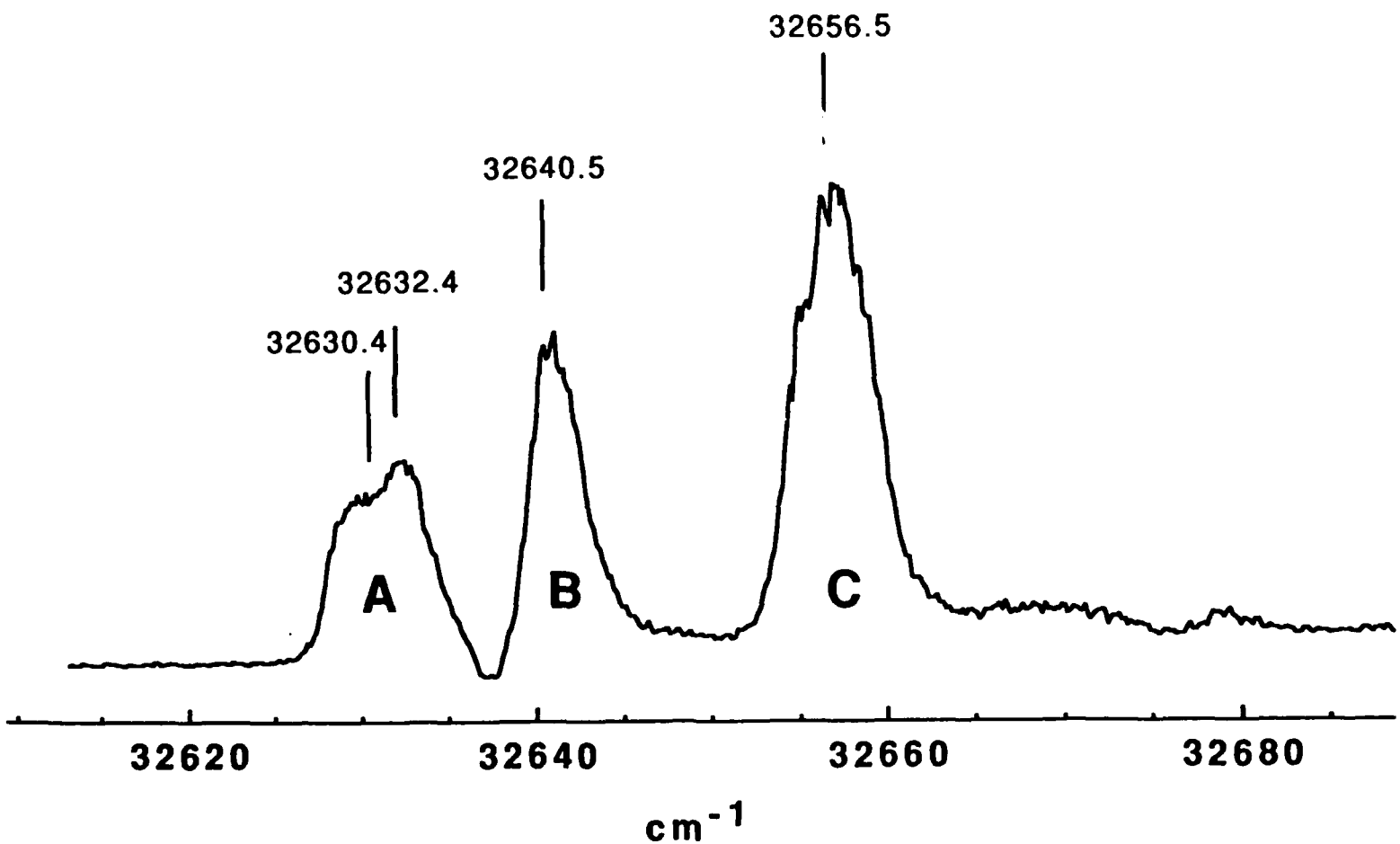
32656.5
32640.5
32632.4
32630.4
A
B
C
32620
32640
32660
32680
cm-1

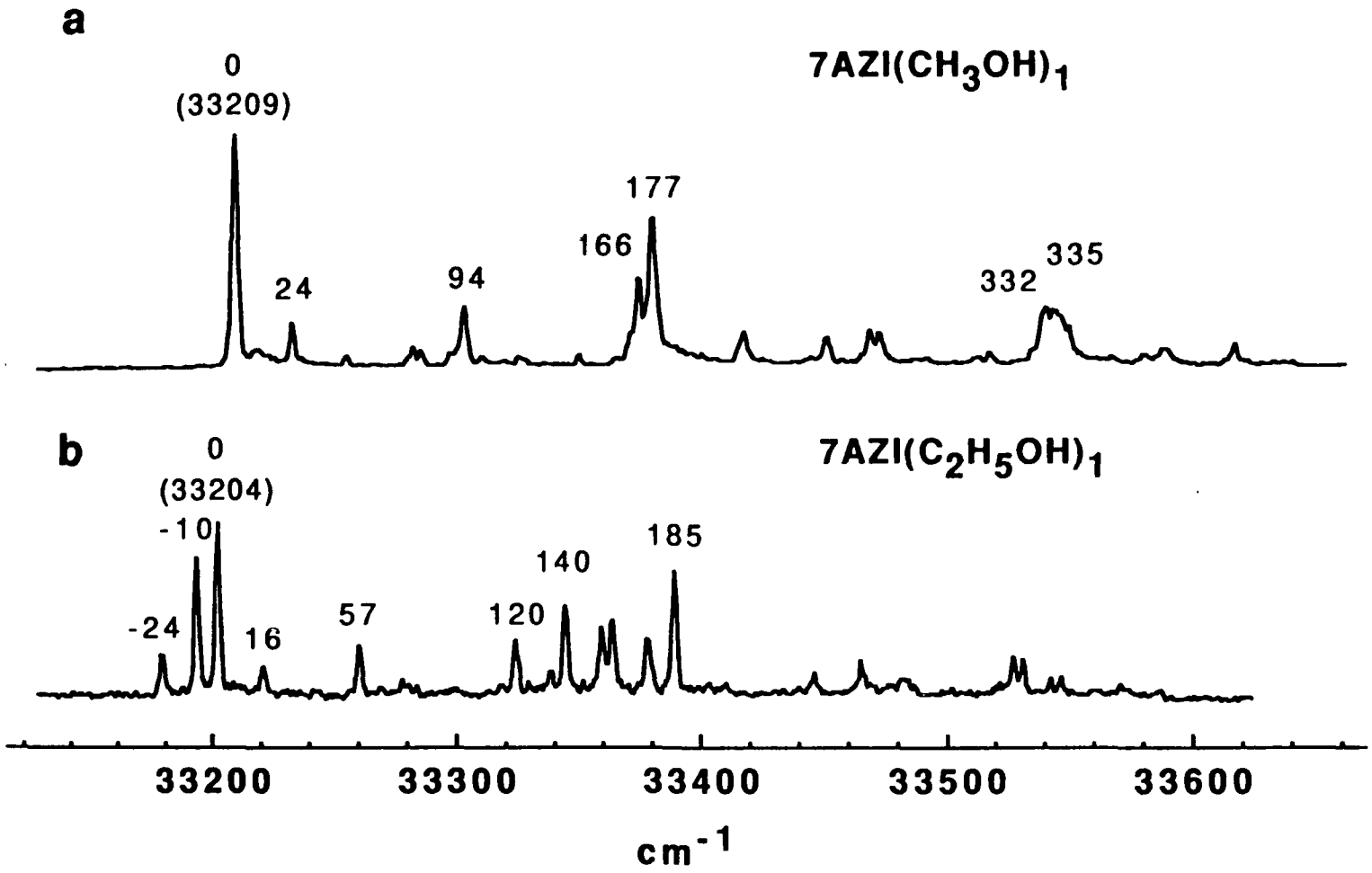
a
0
(33209)
7AZI(CH3OH)1
177
166
24
94
332
335
b
0
(33204)
7AZI(C2H5OH)1
-10
185
140
-24
16
57
120
33200
33300
33400
33500
33600
cm-1

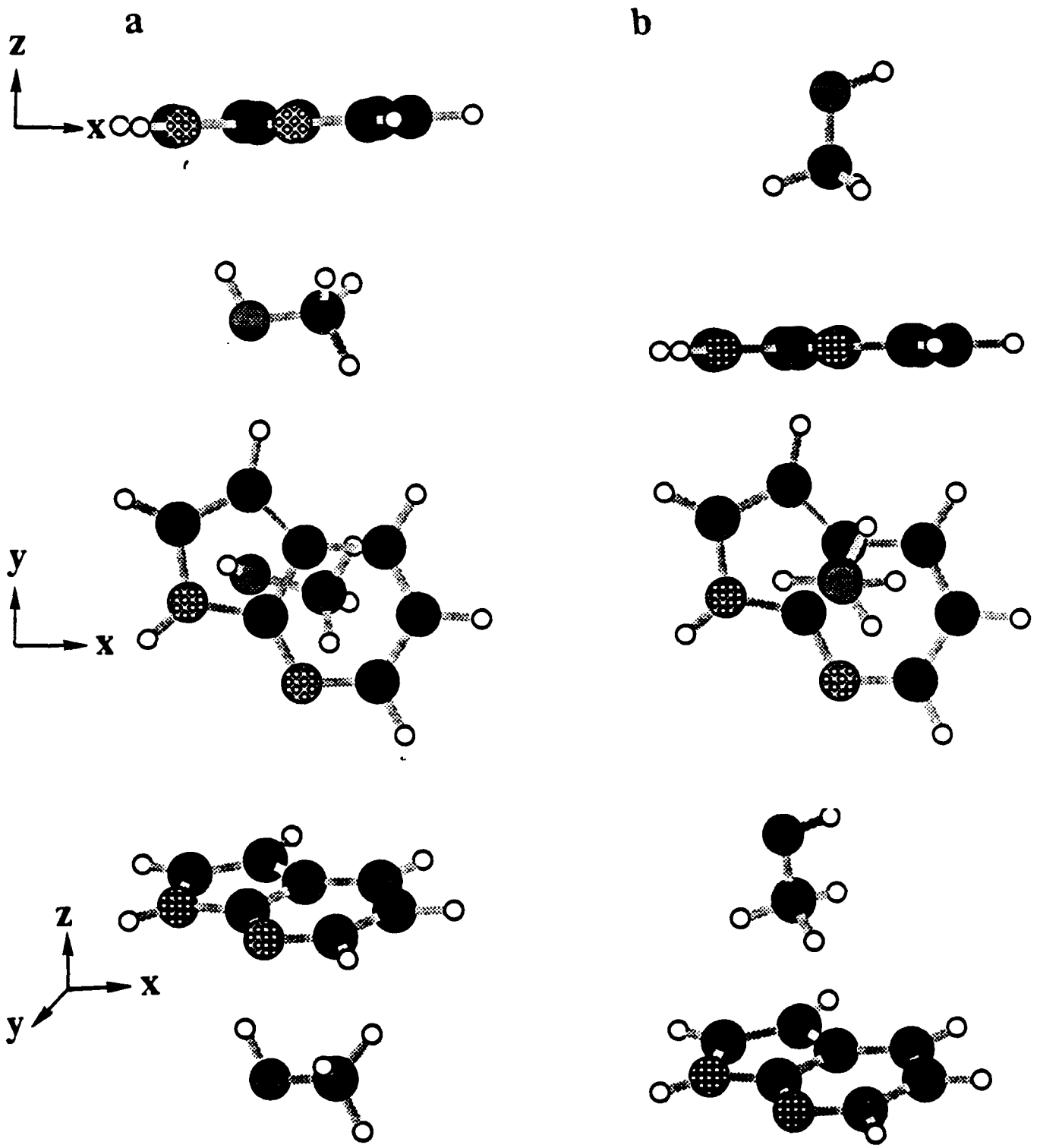

-1100 cm^{-1}(69%)

-1000 cm^{-1}(31%)

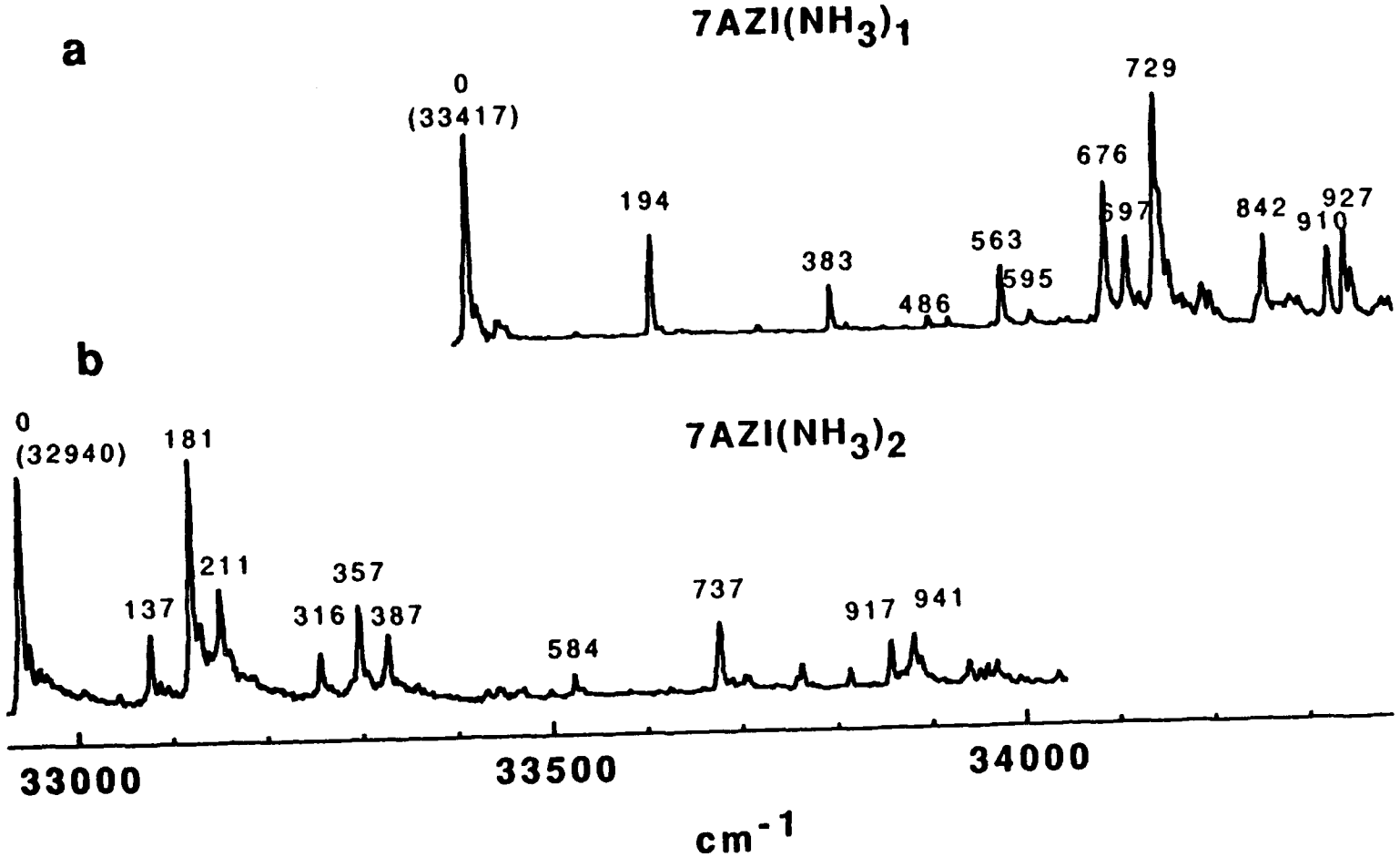
a
7AZI(NH3)1
0
(33417)
194
383
486
563
595
676
697
729
842
910
927
b
7AZI(NH3)2
0
(32940)
137
181
211
316
357
387
584
737
917
941
33000
33500
34000
cm-1

a

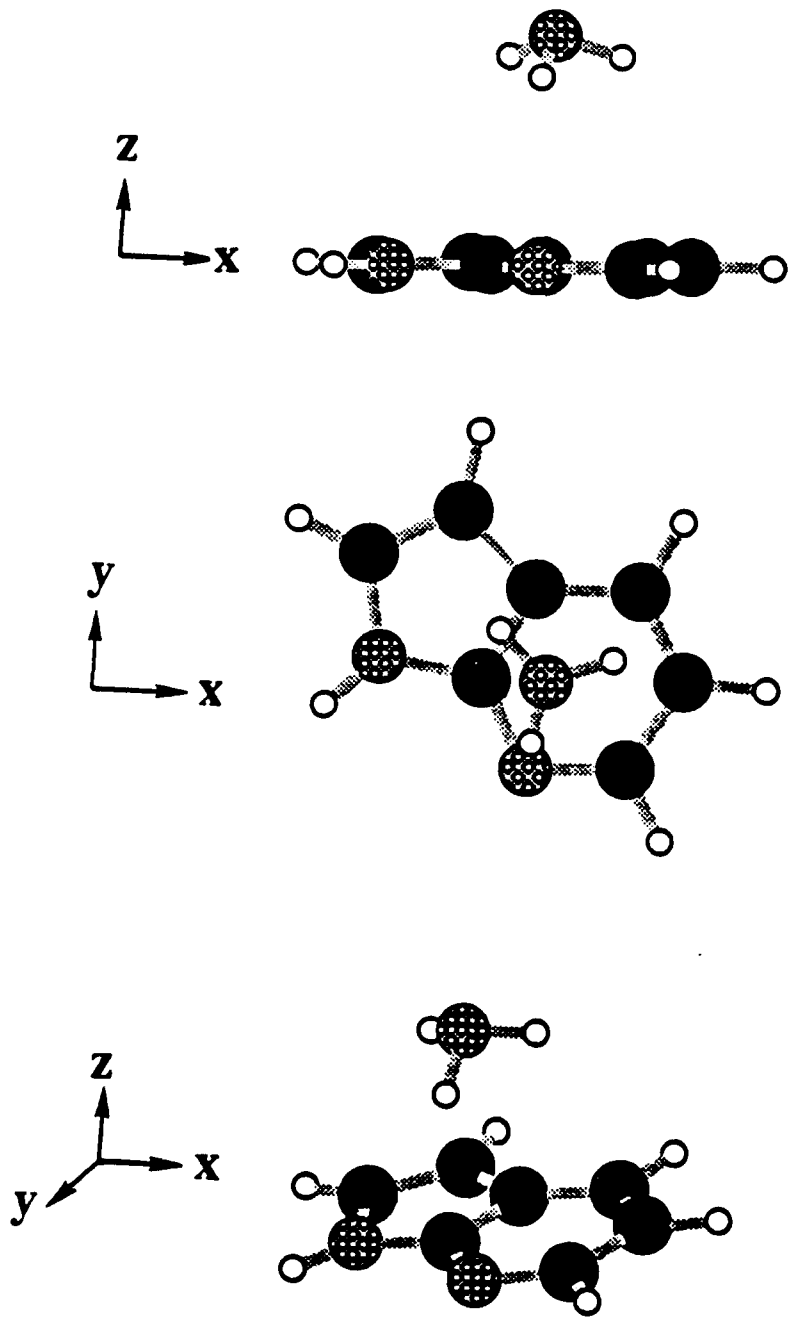

-930 cm-1 (100%)

b

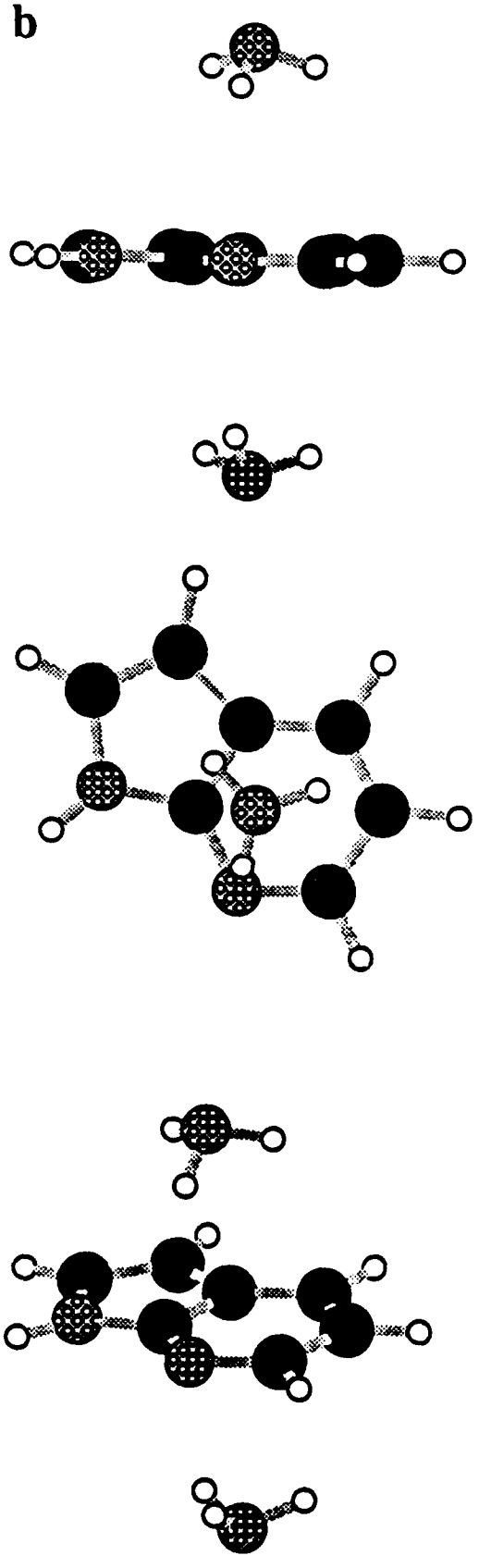

-1850 cm-1 (80%)

c

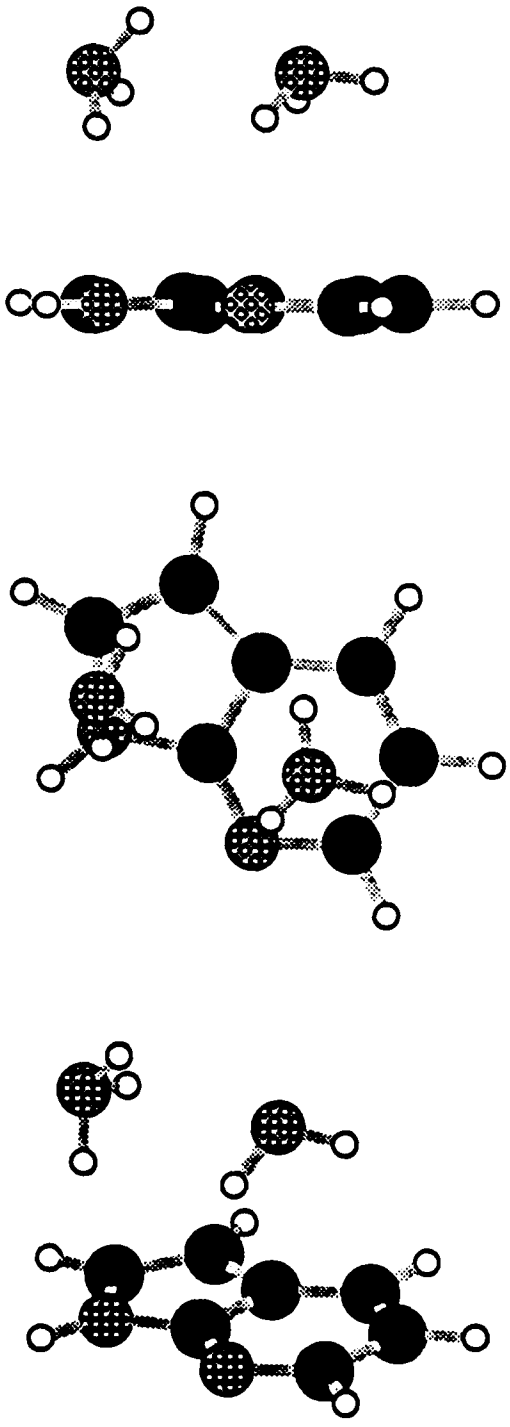

-1950 cm-1 (20%)

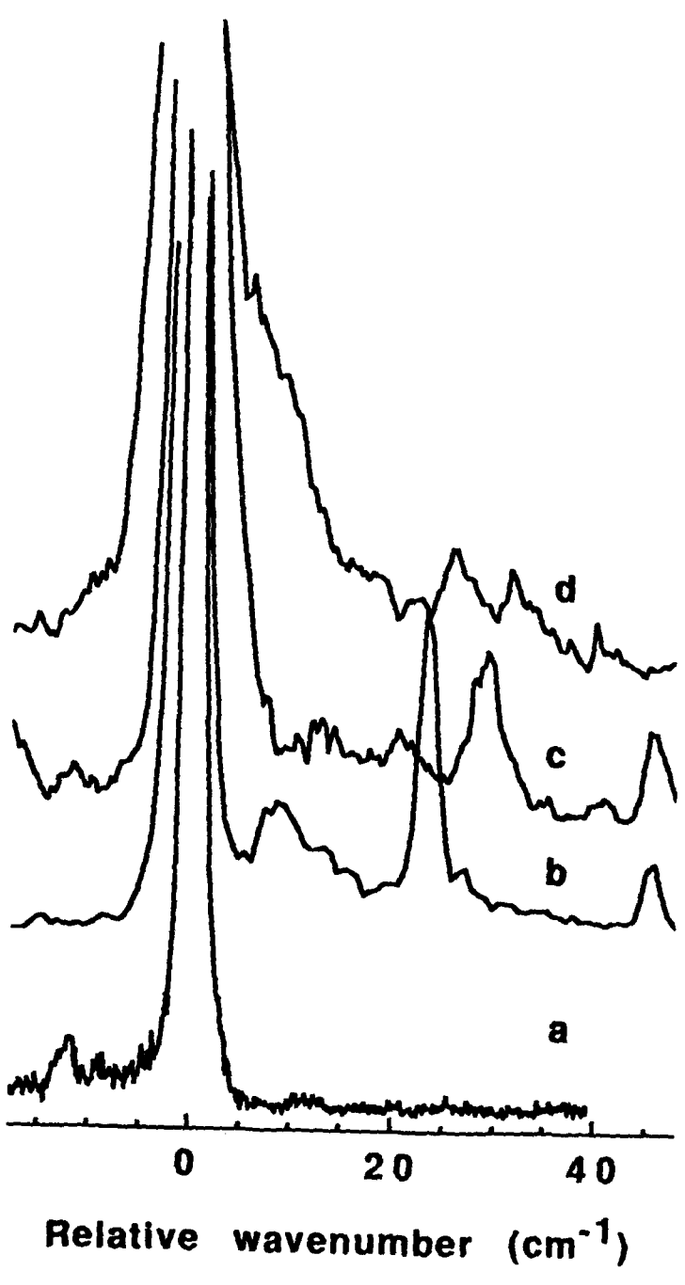
d
c
b
a
0
20
40
Relative wavenumber (cm^{-1})

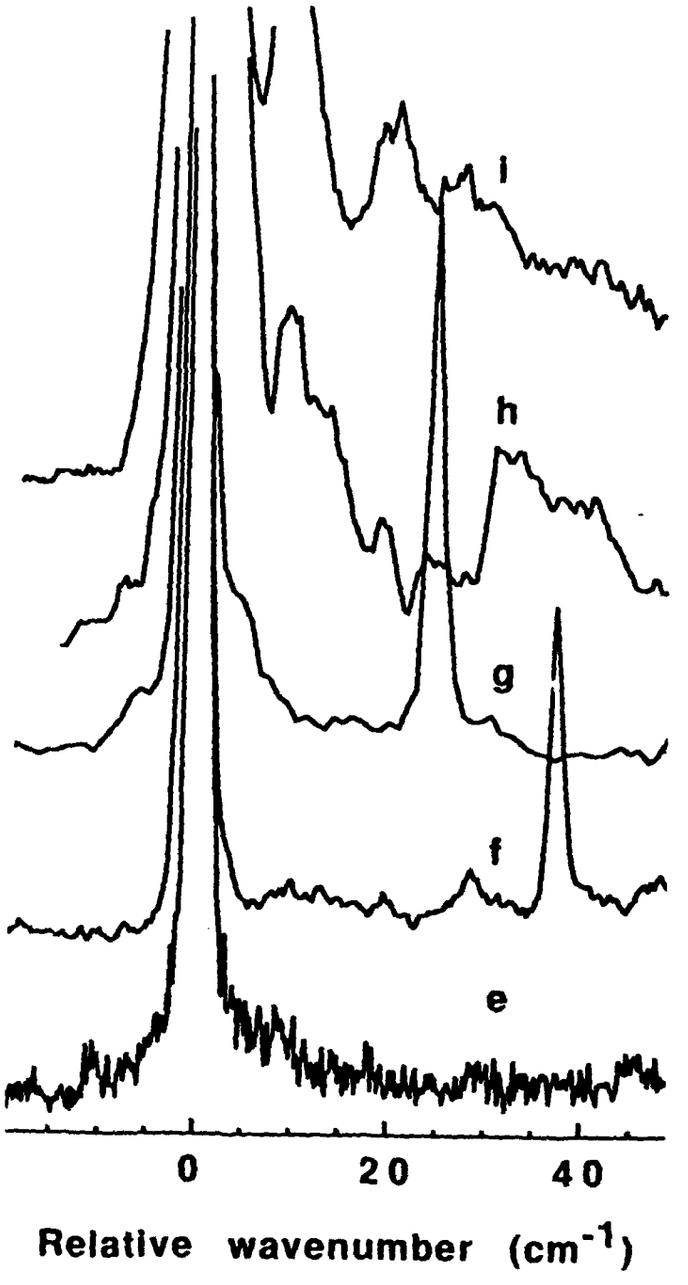
i
h
g
f
e
0
20
40
Relative wavenumber (cm^{-1})

DL/1113/89/1

TECHNICAL REPORT DISTRIBUTION LIST, GENERAL

	No. Copies
Office of Naval Research Chemistry Division, Code 1113 800 North Quincy Street Arlington, VA 22217-5000	3
Commanding Officer Naval Weapons Support Center Attn: Dr. Bernard E. Douda Crane, IN 47522-5050	1
Dr. Richard W. Drisko Naval Civil Engineering Laboratory Code L52 Port Hueneme, California 93043	1
Defense Technical Information Center Building 5, Cameron Station Alexandria, Virginia 22314	2 high quality
David Taylor Research Center Dr. Eugene C. Fischer Annapolis, MD 21402-5067	1
Dr. James S. Murday Chemistry Division, Code 6100 Naval Research Laboratory Washington, D.C. 20375-5000	1
Dr. Ronald L. Atkins Chemistry Division (Code 385) Naval Weapons Center China Lake, CA 93555-6001	1
Chief of Naval Research Special Assistant for Marine Corps Matters Code 00MC 800 North Quincy Street Arlington, VA 22217-5000	1
Dr. Bernadette Eichinger Naval Ship Systems Engineering Station Code 053 Philadelphia Naval Base Philadelphia, PA 19112	1
Dr. Sachio Yamamoto Naval Ocean Systems Center Code 52 San Diego, CA 92152-5000	1
David Taylor Research Center Dr. Harold H. Singerman Annapolis, MD 21402-5067 ATTN: Code 283	1